hep-th/9909122
UTHEP-408
September, 1999

Mordell-Weil Lattice via String Junctions

Mitsuaki Fukae, Yasuhiko Yamada

Department of Mathematics, Kobe University
Rokko, Kobe 657-8501, Japan

Sung-Kil Yang

Institute of Physics, University of Tsukuba
Ibaraki 305-8571, Japan

Abstract

We analyze the structure of singularities, Mordell-Weil lattices and torsions of a rational elliptic surface using string junctions in the background of 12 7-branes. The classification of the Mordell-Weil lattices due to Oguiso-Shioda is reproduced in terms of the junction lattice. In this analysis an important role played by the global structure of the surface is observed. It is then found that the torsions in the Mordell-Weil group are generated by the fraction of loop junctions which represent the imaginary roots of the loop algebra $\widehat{E}_9$. From the structure of the Mordell-Weil lattice we find 7-brane configurations which support non-BPS junctions carrying conserved Abelian charges.

Contents

1 Introduction

In our previous paper [1], and in a related work [2], elliptic curves have been constructed for the 7-brane configurations on which the affine Lie algebras $\widehat{E}_n$ $(1 \leq n \leq 8)$ and $\widehat{\widehat{E}}_n$ $(n = 0, 1)$ are realized. Upon deriving these curves from a rational elliptic surface S, we recognize that the brane picture is very efficient to deal with the geometry of S. In this construction, however, we have only probed the *local* geometry of S with the aid of the 7-brane technology. Our purpose in this paper is to show that 7-branes and string junctions stretched among them precisely capture the *global* structure of a rational elliptic surface.

To explain what kind of global structures we will discuss, let us start with briefly reviewing the heterotic string/F-theory duality. Duality between F-theory on an elliptic $K3$ surface S_F and the heterotic string theory on a two-torus T^2 has been the source of inspiring various duality relations in lower dimensions [3, 4, 5]. In the type IIB picture, singularities of S_F are described in terms of coalescing 7-branes which are in general mutually non-local. The sub-lattice $\Gamma^{18,2}$ of the 22-dimensional homology lattice $\Gamma^{19,3}$ of

$K3$ is spanned by junctions stretched among 7-branes [6]. When the size of T^2 is very large, S_F can be viewed as consisting of two rational elliptic surfaces S_1, S_2, each of which may be associated to one of the heterotic $E_8 \times E_8$ gauge groups [7]. More precisely, in this regime, S_1 and S_2 intersect along an elliptic curve E_* whose complex structure is identified as that of T^2 on the heterotic side. While keeping E_* fixed, then, deformations of the complex structure of S_i are dual to deformations of the corresponding E_8 bundle on T^2 [7, 8].

The gauge symmetry in the heterotic string is now understood in terms of shrinking two-cycles in S_i, or equivalently coalescing 7-branes, on the F-theory side. As found in [9, 10], while the resulting singularity fixes the root lattice, and hence the gauge symmetry *algebra*, the torsion part of the Mordell-Weil group plays a crucial role to determine the gauge *group*. The Mordell-Weil group, as will be described in more detail in the text, is an Abelian group generated by rational sections of the elliptic fibration, and decomposed into its free part and its torsion part. When the torsion part is non-trivial the corresponding gauge group acquires non-trivial π_1, and thus there appears non-simply-connected gauge groups [10].

Thus it is seen that the Mordell-Weil group reflects a global structure of a rational elliptic surface. Furthermore it is known that the Mordell-Weil group equipped with a natural bilinear pairing possesses the lattice structure which is referred to as the Mordell-Weil lattice [11]. The classification of the Mordell-Weil lattice of a rational elliptic surface has already been completed, thanks to Oguiso-Shioda [12].

In this paper, describing the singularity structures of a rational elliptic surface S in terms of 12 7-branes with trivial total monodromy, we will show that the junction lattices on the 7-brane backgrounds precisely produce all the Mordell-Weil lattices of S as listed in [12]. Especially the torsion elements are found to be identified as the "fraction" of global loop junctions which, on the other hand, are related to the imaginary roots of E-type affine Lie algebras.

This paper is organized as follows: In section 2, we introduce some elementary arithmetic of elliptic curves and the notion of the Mordell-Weil group of S using several explicit examples of S presented as elliptic curves. In section 3, after a short review of 7-branes and junctions, we determine the brane configurations which describe the structure of

the Mordell-Weil lattice given in [12]. In this calculation we recognize a non-trivial role played by the global structure of the surface. In section 4, the charge integrality condition is re-considered to obtain the weight lattice and torsions from string junctions. In particular, torsions are expressed as fractional loop junctions. Finally we discuss possibly stable non-BPS states in F-theory on $K3$ on the basis of the structure of the Mordell-Weil lattice.

2 Preliminaries

2.1 Mordell-Weil group

Consider an elliptic curve E defined over $\mathbf{Q}$

$$y^2 = 4x^3 - g_2 x - g_3, \qquad g_2,\ g_3 \in \mathbf{Q}. \tag{2.1}$$

Any cubic in $\mathbf{P}^2$ can be transformed into this canonical form. A point $P = (x, y)$ on E is called rational point if $x, y \in \mathbf{Q}$, the totality of which is denoted as $E(\mathbf{Q})$. Determination of the structure of $E(\mathbf{Q})$ is a deep arithmetic problem. The fundamental fact is that $E(\mathbf{Q})$ has a structure of an Abelian group, known as the Mordell-Weil group [13].

In order to see the group law explicitly, let us recall that a point $P = (x, y)$ on E is parametrized by the Weierstrass $\wp$-function as $x = \wp(t)$, $y = \wp'(t)$. The addition formulae for $\wp$ read

$$\begin{aligned}
\wp(s+t) &= -\wp(s) - \wp(t) + \frac{1}{4}\left(\frac{\wp'(s) - \wp'(t)}{\wp(s) - \wp(t)}\right)^2, \\
\wp'(s+t) &= -\wp'(s) - \wp'(t) + \frac{1}{4}\left(\frac{\wp'(s) - \wp'(t)}{\wp(s) - \wp(t)}\right)^3 + 3\frac{\wp(s)\wp'(t) - \wp(t)\wp'(s)}{\wp(s) - \wp(t)}.
\end{aligned} \tag{2.2}$$

It is obvious that, given $P_i = (x_i, y_i) = (\wp(t_i), \wp'(t_i)) \in E(\mathbf{Q})$ with $i = 1, 2$, the "sum" $P_3 = P_1 + P_2$ defined by $P_3 = (x_3, y_3) = (\wp(t_1 + t_2), \wp'(t_1 + t_2))$ is also in $E(\mathbf{Q})$. The special point at infinity $O = (\infty, \infty)$ is regarded as the unit of this addition. The inverse of $P = (x, y)$ is given by $-P = (x, -y)$.

When the curve E is expressed as a complex torus $E_\tau = \mathbf{C}/(\mathbf{Z} + \tau\mathbf{Z})$, the addition is nothing but the usual sum of complex numbers $t_i \in E_\tau$. Note that if $t_1 + t_2 + t_3 = 0$ in

E_τ then

$$\det \begin{vmatrix} \wp(t_1) & \wp'(t_1) & 1 \\ \wp(t_2) & \wp'(t_2) & 1 \\ \wp(t_3) & \wp'(t_3) & 1 \end{vmatrix} = 0. \tag{2.3}$$

This means that three distinct points $P_i \in E$ satisfy $P_1 + P_2 + P_3 = 0$ if and only if they are on the same line. This geometric rule of the addition, classically known to Fermat and Euler, is applicable for any cubic which is not necessarily in the canonical form (2.1).

Mordell's theorem says that the group $E(\mathbf{Q})$ is finitely generated,

$$E(\mathbf{Q}) \equiv \mathbf{Z}^{\oplus r} \oplus E(\mathbf{Q})_{\rm tor}, \tag{2.4}$$

where the torsion part $E(\mathbf{Q})_{\rm tor}$ is generated by (at most two) generators $P \in E(\mathbf{Q})$ such that $mP = O$ for some $m \in \mathbf{Z}_{>0}$ (see [10] and references therein).

2.2 Elliptic surfaces

What we have described in the previous subsection can be readily generalized for other field K than $\mathbf{Q}$. The relevant case for our analysis in this paper is that K is a field of rational functions of one variable, namely $K = \mathbf{C}(z) = \{\, a(z)/b(z) \mid a(z), b(z) \text{ polynomials in } z\}$. Then the curve

$$y^2 = x^3 + f(z)x + g(z), \tag{2.5}$$

where $f(z)$, $g(z) \in K$, represents an elliptic surface S over $\mathbf{P}^1$ which is a family of elliptic curves $E = \{\, (x, y) \,\}$ parametrized by $z \in \mathbf{P}^1$. Every elliptic surface over $\mathbf{P}^1$ with section can be recast in this form. At the point z on $\mathbf{P}^1$ where the discriminant $\Delta = 4f(z)^3 + 27g(z)^2$ vanishes, the fiber becomes singular. Possible singular fibers were classified by Kodaira, according to which the blowing-up diagram of each singularity is represented by the Dynkin diagram of A, D and E type [14]. In the IIB brane picture, the singularities correspond to the coinciding 7-branes [3].

Now, a point P in the Mordell-Weil group $E(K)$ is a solution $P = (x(z), y(z))$ of (2.5) such that $x(z)$, $y(z) \in K$. In view of the elliptic surface S, a point $P \in E(K)$ is a rational section of the elliptic fibration. Applying the addition formulae (2.2) fiberwise, we see that $E(K)$ has a structure of an Abelian group.

In the following let us take several examples of elliptic surfaces and compute rational sections to show the Abelian group property explicitly. We note in passing that determining sections of elliptic surfaces is essential when one constructs the Seiberg-Witten differential in $\mathcal{N}=2$ supersymmetric gauge theories with matters [15, 16, 17]. In each example below, No.$\sharp$ refers to the entry $\sharp$ of Table 2 which will appear in section 3.

Example. (No.72) : $\mathcal{N}=2$ $SU(2)$ theory with massless $N_f=3$ flavors [15]

$$y^2 = x^2(x-z) - \frac{\Lambda_3^2}{64}(x-z)^2. \tag{2.6}$$

The discriminant is $\Delta = \Lambda_3^2(256z-\Lambda_3^2)z^4/4096$ and the singularities are given by

$$A_3 : (z=0), \qquad D_5 : (z=\infty), \qquad A_0 : (z=\Lambda_3^2/256). \tag{2.7}$$

This curve has four sections generated by a single element P,

$$\begin{aligned} P &= \left(0,\ -\frac{i\Lambda_3}{8}z\right), \qquad & 2P &= (z,\ 0)\,, \\ 3P &= \left(0,\ \frac{i\Lambda_3}{8}z\right), \qquad & 4P &= O = (\infty,\infty). \end{aligned} \tag{2.8}$$

Hence the Mordell-Weil group consists of the torsion part only, *i.e.* $E(K) = \mathbf{Z}/4\mathbf{Z}$.

Example. (No.66) : Massless $\widehat{E}_3$ curve [18, 1, 2]

$$y^2 = x^3 + (z^2+10z-23)x^2 + 128(1-z)x. \tag{2.9}$$

The discriminant is $\Delta = -16384(z+1)^3(z-1)^2(z+17)$ and the singularities are

$$A_5 : (z=\infty), \qquad A_2 : (z=-1), \qquad A_1 : (z=1), \qquad A_0 : (z=-17). \tag{2.10}$$

This curve has six sections generated by a single element P,

$$\begin{aligned} P &= (8(1-z),\ -8(1-z^2)), \qquad & 2P &= (16,\ -16(1+z)), \\ 3P &= (0,\ 0), & 4P &= (16,\ 16(1+z)), \\ 5P &= (8(1-z),\ 8(1-z^2)), \qquad & 6P &= O = (\infty,\infty). \end{aligned} \tag{2.11}$$

Hence we have $E(K) = \mathbf{Z}/6\mathbf{Z}$.

Example. (No.44 and its degeneration to No.70) : Massive and massless $\widehat{E}_1$ curve [18, 1, 2]

The massive $\widehat{E}_1$ curve reads

$$y^2 = x^3 + \left(z^2 - 2(p + \frac{16}{p})z + p^2 - 224\right) x^2 + \frac{65536}{p^2}x. \tag{2.12}$$

The discriminant is

$$\Delta = -4294967296(z-p-16)(z-p+16)(pz-p^2+16p-32)(pz-p^2-16p-32)/p^6. \tag{2.13}$$

The singularities are

$$\begin{aligned} A_7 \quad &: \quad (z = \infty), \\ A_0 + A_0 + A_0 + A_0 \quad &: \quad (z = p \pm 16,\ p + \frac{32}{p} \pm 16). \end{aligned} \tag{2.14}$$

The Mordell-Weil group $E(K)$ is generated by

$$\begin{aligned} P = (0,\ 0), \qquad Q &= \left(256,\ 256z - 256\frac{16+p^2}{p}\right), \\ R &= \left(\frac{256}{p^2},\ \frac{256}{p^2}z - 256\frac{16+p^2}{p^3}\right). \end{aligned} \tag{2.15}$$

Since $2P = O$, $Q + R = P$ we have $E(K) = \mathbf{Z} \oplus \mathbf{Z}/2\mathbf{Z}$ where the free part $\mathbf{Z}$ and the torsion part $\mathbf{Z}/2\mathbf{Z}$ are generated by Q and P, respectively.

Under the degeneration at $p = 1$ (massless $\widehat{E}_1$ curve) the discriminant becomes

$$\Delta = -4294967296(z + 15)(z - 49)(z - 17)^2 \tag{2.16}$$

and the singularities are

$$A_7 : (z = \infty), \qquad A_1 : (z = 17), \qquad A_0 + A_0 : (z = -15, 49). \tag{2.17}$$

In this case, we have $Q = R$ and $4Q = 2P = O$, thereby $E(K)$ reduces to $E(K) = \mathbf{Z}/4\mathbf{Z}$.

Example. (No.27) : Massive A_2 curve [17]

$$y^2 = x^3 + ux + v + z^2. \tag{2.18}$$

The discriminant is $\Delta = 27z^4 + 54vz^2 + 4u^3 + 27v^2$ and the singularities are

$$\begin{aligned} E_6 &: (z = \infty), \\ A_0 + A_0 + A_0 + A_0 &: (\Delta(z) = 0), \end{aligned} \tag{2.19}$$

This curve has six fundamental sections,

$$\pm P_i = (a_i, \pm z), \quad i = 1, 2, 3, \tag{2.20}$$

where a_i are determined through $(x-a_1)(x-a_2)(x-a_3) = x^3+ux+v$. These six sections $\pm P_i$ correspond to the six fundamental weights of the A_2 algebra $\pm\Lambda_1$, $\pm(\Lambda_2 - \Lambda_1)$ and $\pm(-\Lambda_2)$. By addition formulae (2.2), one can generate a section $P_{l,m}$ corresponding to a weight $\lambda = l\Lambda_1 + m\Lambda_2$ for each $(l, m) \in \mathbf{Z}^{\oplus 2}$. Thus we see that $E(K) \equiv \mathbf{Z}^{\oplus 2}$ as an abstract group, but it has a more detailed structure as a lattice $E(K) = A_2^*$. Here a "lattice" is introduced as a free Abelian group $L = \mathbf{Z}^{\oplus r}$ with a symmetric bilinear form $(\ ,\ ) : L \otimes L \to \mathbf{Z}$. The equality $E(K) = A_2^*$ means the isomorphism as a lattice. The bilinear form on $E(K)$ is defined by the "height pairing" which can be explicitly evaluated in terms of an intersection pairing on an elliptic surface S, see next section.

Finally it is mentioned that, extending the computation in [17], we have shown that the Seiberg-Witten differential for the curve (2.18) can be constructed so that it has the poles with residues located on sections (3.6). The details may appear elsewhere.

3 Mordell-Weil lattice vs. junction lattice

3.1 Mordell-Weil lattice

Let us start with recapitulating what we have discussed in the previous section, then we introduce the notion of the Mordell-Weil lattice, following [11]. We take an elliptic curve E defined over a field K

$$y^2 = x^3 + fx + g, \qquad f,\ g \in K. \tag{3.1}$$

A point $P = (x, y) \in K^2$ on the curve E is called K-rational point. Let $E(K)$ denote a set of all the K-rational points plus the point at infinity $O = (\infty, \infty)$. For given

fiber type	singularity lattice	7-branes
I_n $(n \geq 1)$	A_{n-1}	$\mathbf{A}^n = \mathbf{A_{n-1}}$
$\mathrm{II}, \mathrm{III}, \mathrm{IV}$ $(n = 0, 1, 2)$	A_n	$\mathbf{A}^{n+1}\mathbf{C} = \mathbf{H_n}$
I_n^* $(n \geq 0)$	D_{n+4}	$\mathbf{A}^{n+4}\mathbf{BC} = \mathbf{D_{n+4}}$
$\mathrm{II}^*, \mathrm{III}^*, \mathrm{IV}^*$ $(n = 8, 7, 6)$	E_n	$\mathbf{A}^{n-1}\mathbf{BC}^2 = \mathbf{E_n}$

Table 1: Kodaira classification, ADE singularities and 7-branes.

$P_i = (x_i, y_i) \in E(K)$ with $i = 1, 2$, the third point $P_3 = P_1 + P_2 = (x_3, y_3) \in E(K)$ is defined by

$$x_3 = -x_1 - x_2 + m^2, \qquad y_3 = -m(x_3 - x_1) - y_1, \tag{3.2}$$

where

$$m = \begin{cases} (y_1 - y_2)/(x_1 - x_2), & \text{if } P_1 \neq P_2, \\ (3x_1^2 + f)/(2y_1), & \text{if } P_1 = P_2. \end{cases} \tag{3.3}$$

With respect to this addition law, $E(K)$ has a structure of Abelian group, called the Mordell-Weil group. The point at infinity $O \in E(K)$ is the unit of this addition.

In this paper we are mainly concerned with the case of $K = \mathbf{C}(z)$ (the field of rational functions on z). Then (3.1) is naturally considered as an elliptic surface S over $\mathbf{P}^1$, for which the points $P = (x(z), y(z)) \in E(K)$ represent the rational sections of this fibration. The Kodaira classification of singular fibers is presented in Table 1. We denote by T the lattice corresponding to the singular fibers.

There exists a deep relation between the singularities T and the sections $E(K)$, reflecting the global structure of the elliptic surface S. The essential idea in studying such relation is to equip $E(K)$ with the lattice structure which can be described in terms of intersections on S.

The lattice structure, or the height pairing $(\ ,\ )$ of the Mordell-Weil group $E(K)$ was introduced by Shioda using the intersection pairing [11]. The Mordell-Weil group equipped with the height pairing is called the Mordell-Weil lattice. In Theorem 8.1 [11], the height pairing (P, Q) for sections $P, Q \in E(K)$ is explicitly calculated as follows:

$$(P, Q) = P \cdot O + Q \cdot O - P \cdot Q + \chi(\mathcal{O}_S) - \sum_v \mathrm{contr}_v(P, Q),$$

$$(P,P) = 2\chi(\mathcal{O}_S) + 2P\cdot O - \sum_v \mathrm{contr}_v(P), \tag{3.4}$$

where $P\cdot Q$ denotes the intersection pairing, $\chi(\mathcal{O}_S)$ is the arithmetic genus of S ($=1$ for rational elliptic surfaces) and contr_v is the local contribution from each singular point v

$$\mathrm{contr}_v(P,Q) = \begin{cases} 0, & \text{if } i=0 \text{ or } j=0, \\ (C_v^{-1})_{ij}, & \text{otherwise} \end{cases} \tag{3.5}$$

and $\mathrm{contr}_v(P) = \mathrm{contr}_v(P,P)$. Here C_v is the Cartan matrix (of finite type) corresponding to the singularity at v and the indices i,j label the components of the singular fibers with which P or Q intersects. The component intersecting with the zero section O is specified by $i=0$.

Example. (No.27 : The massive A_2-curve (2.18) continued)
The rational section $P_{l,m}$ corresponding to a weight vector $\lambda = l\Lambda_1 + m\Lambda_2$ takes the form

$$x(z) = \frac{\phi(z)}{\chi(z)^2}, \qquad y(z) = \frac{\psi(z)}{\chi(z)^3}, \tag{3.6}$$

where $\deg\psi(z) = d_{l,m} = l^2+lm+m^2$, $\deg\chi(z) = \frac{1}{3}d_{l,m} - 1$ [resp. $\frac{1}{3}d_{l,m} - \frac{1}{3}$] and $\deg\phi(z) = \frac{2}{3}d_{l,m}$ [resp. $\frac{2}{3}d_{l,m} - \frac{2}{3}$] for $l \equiv m \pmod 3$ [resp. otherwise]. For this section $P_{l,m}$, the second formula in (3.4) can be checked since we evaluate $(P_{l,m},P_{l,m}) = (l\Lambda_1+m\Lambda_2)^2 = \frac{2}{3}d_{l,m}$, $\mathrm{contr}_{z=\infty}(P_{l,m}) = 0$ [resp. $\frac{4}{3}$] and $O\cdot P_{l,m} = \deg\chi(z)$.*

Noting that the structure of the Mordell-Weil lattice $E(K)$ is essentially determined by the singularity lattice T, Oguiso-Shioda classified the Mordell-Weil lattice $E(K)$ of a rational elliptic surface [12]. This will be described in detail in section 3.3. Our task is now to figure out how the Mordell-Weil lattice $E(K)$ and the singularity lattice T are related to each other in terms of the junctions on rational elliptic surfaces.†

3.2 Brane configurations and junction lattice

We concentrate on a rational elliptic surface S defined by (3.1) where $f = f(z)$ and $g = g(z)$ are some polynomials in z, and $\deg f \le 4$, $\deg g \le 6$ with $\Delta \neq$ constant.

*In the homogeneous coordinates $(X:Y:Z)$, the curve and sections are rewritten as $ZY^2 = X^3 + f(z)XZ^2 + g(z)Z^3$, $P = (X:Y:Z) = (\phi\chi, \psi, \chi^3)$. Hence, the intersection of P with zero-section $O = (0:1:0)$ is given by $\deg\chi(z)$.

†In case of more general elliptic surfaces, elliptic K3 for instance, the junction lattice will contain transcendental cycles also.

Generically there exist 12 singular points z_i where $\Delta(z_i) = 0$. Each singular fiber at $z = z_i$ has a local monodromy $K_{[p_i,q_i]}$ labeled by $p_i, q_i \in \mathbf{Z}$. Here the monodromy matrix takes the form

$$K_{[p,q]} = \begin{pmatrix} 1+pq & -p^2 \\ q^2 & 1-pq \end{pmatrix}, \tag{3.7}$$

corresponding to a vanishing cycle $p\alpha + q\beta$ with α, β being homology cycles of a fiber torus. Physically a singular point is interpreted as the position of a 7-brane $\mathbf{X_{[p,q]}}$ on which a (p,q)-string with a boundary homologous to $p\alpha + q\beta$ can end [3]. Among various (p,q) 7-branes $\mathbf{X_{[p,q]}}$ it is convenient to express the representative ones as $\mathbf{X_{[1,0]}} = \mathbf{A}, \mathbf{X_{[1,-1]}} = \mathbf{B}, \mathbf{X_{[1,1]}} = \mathbf{C}$. The Kodaira singularities can be then described as a coalescence of collapsible sub-configurations of 7-branes, see Table 1 [19, 20].

To specify a brane configuration, we place the 12 branes, say, on the real axis of the z-plane and draw downwards the branch cuts emanating from the branes. Thus, for a brane configuration

$$\mathbf{X_{[p_1,q_1]}X_{[p_2,q_2]}} \cdots \mathbf{X_{[p_{12},q_{12}]}}, \tag{3.8}$$

we have the total monodromy

$$K = K_{[p_{12},q_{12}]} \cdots K_{[p_2,q_2]} K_{[p_1,q_1]} \tag{3.9}$$

which should be trivial, *i.e.* $K = 1$, to describe a rational elliptic surface S. A standard realization of such a brane configuration is [6]

$$\widehat{\mathbf{E}}_\mathbf{9} = \mathbf{A}^8\mathbf{BCBC}. \tag{3.10}$$

A topological configuration of strings (or string junctions) associated to the branes can be parameterized as

$$\mathbf{J} = \sum_{i=1}^{12} Q_i \mathbf{s}_i \qquad \text{or} \qquad \mathbf{J} = (Q_1, Q_2, \ldots, Q_{12}), \tag{3.11}$$

where $\mathbf{s}_i$ stands for the outgoing (p_i, q_i)-string starting at $\mathbf{X_{[p_i,q_i]}}$ and Q_i is the net number of outgoing (p_i, q_i)-strings. By definition the charges Q_i must be integral and are called the invariant charges [19]. The total (p,q) charges of a string junction are

$$(p,q) = \sum_{i=1}^{12} Q_i (p_i, q_i). \tag{3.12}$$

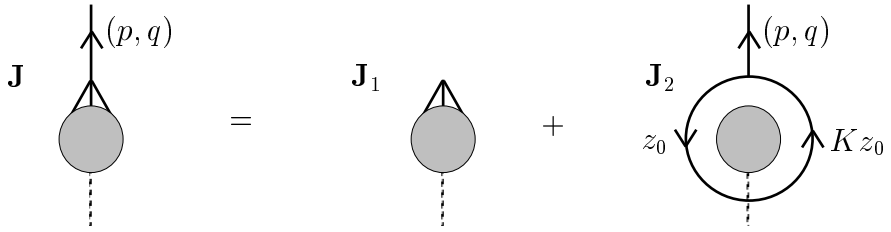

Figure 1: A string junction.

A junction represents a closed two-cycle in S if and only if its total charges vanish.

A (p,q)-junction $\mathbf{J}$ is in general decomposed into two pieces $\mathbf{J}_1$, $\mathbf{J}_2$ as depicted in Figure 1. If $\mathbf{J}$ is a singlet with respect to the symmetry realized on the branes, then $\mathbf{J}_1 = 0$. The charge $\mathbf{z}_0 = (r,s)$ of the tadpole loop $\mathbf{J}_2$ is determined by charge conservation at the trivalent vertex. When the tadpole loop goes around the $\mathbf{A_n}$, $\mathbf{D_n}$ and $\mathbf{E_n}$ branes of Table 1, the loop charges (r,s), invariant charges Q_i and outgoing charges (p,q) are related as follows:

$$\begin{aligned}
\mathbf{A_n}: \quad & \boldsymbol{\delta}_{r,s} = -s(\mathbf{s}_1 + \cdots + \mathbf{s}_{n+1}), \\
& (p,q) = (-(n+1)s,\, 0), \qquad (3.13) \\
\mathbf{D}_n: \quad & \boldsymbol{\delta}_{r,s} = -s(\mathbf{s}_1 + \cdots + \mathbf{s}_n) - (r-(n-1)s)\mathbf{s}_{n+1} - (r-(n-3)s)\mathbf{s}_{n+2}, \\
& (p,q) = (-2r + (n-4)s,\, -2s), \qquad (3.14) \\
\mathbf{E_n}: \quad & \boldsymbol{\delta}_{r,s} = -s(\mathbf{s}_1 + \cdots + \mathbf{s}_{n-1}) - (r-(n-2)s)\mathbf{s}_{n+1} - (r-(n-4)s)(\mathbf{s}_{n+1} + \mathbf{s}_{n+2}), \\
& (p,q) = (-3r + (2n-9)s,\, -r + (n-6)s). \qquad (3.15)
\end{aligned}$$

It should be remembered that if one employs a different 7-brane configuration from the ones given in Table 1 to describe the ADE singularities, the assignment of the (r,s) charges will also change.

The junctions form a lattice which is endowed with a symmetric intersection pairing defined by [19]

$$\begin{aligned}
& (\mathbf{s}_i, \mathbf{s}_i) = -1, \\
& (\mathbf{s}_i, \mathbf{s}_j) = (\mathbf{s}_j, \mathbf{s}_i) = \frac{1}{2}\left(p_i q_j - p_j q_i\right), \quad \text{for } i < j. \qquad (3.16)
\end{aligned}$$

For the sub-configurations in Table 1, the junction lattice with $(p,q) = 0$ is known to

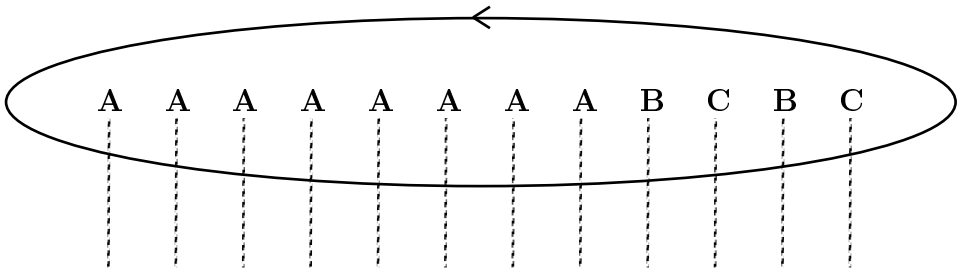

Figure 2: A loop junction.

be isomorphic to the corresponding root lattice [19]. In these cases, the root junctions represent the BPS strings responsible for the symmetry enhancement.

For $\widehat{\mathbf{E}}_\mathbf{9}$ the junction lattice forms an indefinite lattice with signature $(2+, 10-)$. Under the condition that the total (p, q) charges (3.12) vanish, this lattice reduces to the semi-definite one isomorphic to

$$\mathbf{Z}\boldsymbol{\delta}_1 \oplus \mathbf{Z}\boldsymbol{\delta}_2 \oplus (-E_8). \tag{3.17}$$

Here $\boldsymbol{\delta}_1$ and $\boldsymbol{\delta}_2$ are the null junctions. A choice of basis is

$$\begin{aligned} \boldsymbol{\delta}_1 &= (0,0,0,0,0,0,0,0,-1,-1,1,1), \\ \boldsymbol{\delta}_2 &= (-1,-1,-1,-1,-1,-1,-1,-1,7,5,-3,-1). \end{aligned} \tag{3.18}$$

The $\boldsymbol{\delta}_1$, $\boldsymbol{\delta}_2$ junctions are expressed as loops of $(1,0)$, $(0,1)$ strings, respectively, surrounding the $\widehat{\mathbf{E}}_\mathbf{9}$ branes (3.10) counterclockwise, see Figure 2. These null junctions represent two imaginary roots of the loop algebra $\widehat{E}_9$ [6] and will play a crucial role in our study of torsions in section 4.

3.3 Mordell-Weil lattice from junctions

A rational elliptic surface S is a special kind of 9 points blown-up of $\mathbf{P}^2$ and $b_2 = \dim H_2(S) = 10$. $H_2(S)$ is a unimodular Lorentzian lattice with signature $(1+, 9-)$. Let O and F be a class of zero section and generic fiber. Their intersections are $O \cdot O = -1$, $O \cdot F = 1$ and $F \cdot F = 0$. The orthogonal complement of $\langle O, F \rangle$ in $H_2(S)$ is isomorphic to $-E_8$.

Some elements of $H_2(S)$ appear as components of singular fibers. They generate the root lattice corresponding to the singularity type. Let $T \subset E_8$ be the lattice generated by

the components of singular fibers. Theorem 10.3 in [11] states that the structure of the Mordell-Weil group of the rational elliptic surface S is described as

$$E(K) \simeq L^* \oplus (T'/T), \tag{3.19}$$

where L^* is the dual of $L = T^\perp$ (in E_8) and $T' = T \otimes \mathbf{Q} \cap E_8$. From (3.19) the torsion subgroup $E(K)_{\rm tor}$ of $E(K)$ is read off as $E(K)_{\rm tor} \simeq T'/T$, and hence $E(K)/E(K)_{\rm tor} \simeq L^*$. According to this theorem, the computation of $E(K)$ is reduced to the embedding of lattice T in E_8.

In [12] all the possible structures of T and $E(K)$ are classified. They are listed in Table 2 where $r = \operatorname{rank} E(K)$.[¶] In the last column for $E(K)$, $\langle k \rangle$ denotes a rank one lattice $\mathbf{Z}\,x$ with $(x,x) = k$ and

$$\Lambda_{(12)} = \tfrac{1}{6}\begin{pmatrix} 2 & 1 & 0 & -1 \\ 1 & 5 & 3 & 1 \\ 0 & 3 & 6 & 3 \\ -1 & 1 & 3 & 5 \end{pmatrix}, \qquad \Lambda_{(17)} = \tfrac{1}{10}\begin{pmatrix} 3 & 1 & -1 \\ 1 & 7 & 3 \\ -1 & 3 & 7 \end{pmatrix},$$
$$\Lambda_{(19)} = \tfrac{1}{12}\begin{pmatrix} 7 & 1 & 2 \\ 1 & 7 & 2 \\ 2 & 2 & 4 \end{pmatrix}, \qquad \Lambda_{(23)} = \tfrac{1}{6}\begin{pmatrix} 2 & 1 \\ 1 & 2 \end{pmatrix}, \tag{3.20}$$
$$\Lambda_{(25)} = \tfrac{1}{7}\begin{pmatrix} 2 & 1 \\ 1 & 4 \end{pmatrix}, \qquad \Lambda_{(31)} = \tfrac{1}{15}\begin{pmatrix} 2 & 1 \\ 1 & 8 \end{pmatrix},$$
$$\Lambda_{(33)} = \tfrac{1}{10}\begin{pmatrix} 2 & 1 \\ 1 & 3 \end{pmatrix}.$$

To understand this result of [12] in terms of junctions, we have to solve the following two problems:

(1) Find the collapsible sub-configurations of 7-branes which support the singularity lattice T as the junction lattice.

(2) Compute the lattice L using string junctions on the 7-brane backgrounds.

The problem (1) is solved by finding a suitable rearrangement of the $\widehat{\mathbf{E}}_\mathbf{9}$ configurations (3.10) with the use of the brane move [21, 20]

$$\mathbf{X}_{\mathbf{z}_i}\mathbf{X}_{\mathbf{z}_{i+1}} = \mathbf{X}_{\mathbf{z}'_i}\mathbf{X}_{\mathbf{z}'_{i+1}}, \tag{3.21}$$

[¶] $E(K) = A_1^* \oplus \langle 1/6 \rangle$ for No.32 and $(\mathbf{Z}/2\mathbf{Z})^2$ for No.70 in [12] should read $E(K) = \Lambda_{(23)}$ and $\mathbf{Z}/4\mathbf{Z}$, respectively.

No.	r	T	branes	$E(K)$
1	8	0	$\mathbf{A}^8\mathbf{BCBC}$	E_8
2	7	A_1	$(\mathbf{A}^2)\mathbf{A}^6\mathbf{BCBC}$	E_7^*
3	6	A_2	$(\mathbf{A}^3)\mathbf{A}^5\mathbf{BCBC}$	E_6^*
4		${A_1}^{\oplus 2}$	$(\mathbf{A}^2)^2\mathbf{A}^4\mathbf{BCBC}$	D_6^*
5	5	A_3	$(\mathbf{A}^4)\mathbf{A}^4\mathbf{BCBC}$	D_5^*
6		$A_2 \oplus A_1$	$(\mathbf{A}^3)(\mathbf{A}^2)\mathbf{A}^3\mathbf{BCBC}$	A_5^*
7		${A_1}^{\oplus 3}$	$(\mathbf{A}^2)^3\mathbf{A}^2\mathbf{BCBC}$	$D_4^* \oplus A_1^*$
8	4	A_4	$(\mathbf{A}^5)\mathbf{A}^3\mathbf{BCBC}$	A_4^*
9		D_4	$(\mathbf{A}^4\mathbf{BC})\mathbf{A}^4\mathbf{BC}$	D_4^*
10		$A_3 \oplus A_1$	$(\mathbf{A}^4)(\mathbf{A}^2)\mathbf{A}^2\mathbf{BCBC}$	$A_3^* \oplus A_1^*$
11		${A_2}^{\oplus 2}$	$(\mathbf{A}^3)^2\mathbf{A}^2\mathbf{BCBC}$	$A_2^{*\oplus 2}$
12		$A_2 \oplus {A_1}^{\oplus 2}$	$(\mathbf{A}^3)(\mathbf{A}^2)^2\mathbf{ABCBC}$	$\Lambda_{(12)}$
13		${A_1}^{\oplus 4}$	$(\mathbf{A}^2)^4\mathbf{BCBC}$	$D_4^* \oplus \mathbf{Z}/2\mathbf{Z}$
14		${A_1}^{\oplus 4}$	$(\mathbf{A}^2)^4\mathbf{A}\mathbf{X}_{[\mathbf{2},-\mathbf{1}]}\mathbf{X}_{[\mathbf{1},-\mathbf{2}]}\mathbf{C}$	$A_1^{*\oplus 4}$
15	3	A_5	$(\mathbf{A}^6)\mathbf{A}^2\mathbf{BCBC}$	$A_2^* \oplus A_1^*$
16		D_5	$(\mathbf{A}^5\mathbf{BC})\mathbf{A}^3\mathbf{BC}$	A_3^*
17		$A_4 \oplus A_1$	$(\mathbf{A}^5)(\mathbf{A}^2)\mathbf{ABCBC}$	$\Lambda_{(17)}$
18		$D_4 \oplus A_1$	$(\mathbf{A}^4\mathbf{BC})(\mathbf{A}^2)\mathbf{A}^2\mathbf{BC}$	$A_1^{*\oplus 3}$
19		$A_3 \oplus A_2$	$(\mathbf{A}^4)(\mathbf{A}^3)\mathbf{ABCBC}$	$\Lambda_{(19)}$
20		${A_2}^{\oplus 2} \oplus A_1$	$(\mathbf{A}^3)^2(\mathbf{A}^2)\mathbf{BCBC}$	$A_2^* \oplus \langle 1/6 \rangle$
21		$A_3 \oplus {A_1}^{\oplus 2}$	$(\mathbf{A}^4)(\mathbf{A}^2)^2\mathbf{BCBC}$	$A_3^* \oplus \mathbf{Z}/2\mathbf{Z}$
22		$A_3 \oplus {A_1}^{\oplus 2}$	$(\mathbf{A}^4)(\mathbf{A}^2)^2\mathbf{A}\mathbf{X}_{[\mathbf{2},-\mathbf{1}]}\mathbf{X}_{[\mathbf{1},-\mathbf{2}]}\mathbf{C}$	$A_1^{*\oplus 2} \oplus \langle 1/4 \rangle$
23		$A_2 \oplus {A_1}^{\oplus 3}$	$(\mathbf{A}^3)(\mathbf{A}^2)^3\mathbf{X}_{[\mathbf{2},-\mathbf{1}]}\mathbf{X}_{[\mathbf{1},-\mathbf{2}]}\mathbf{C}$	$A_1^* \oplus \Lambda_{(23)}$
24		${A_1}^{\oplus 5}$	$(\mathbf{A}^2)^2(\mathbf{B}^2)^2(\mathbf{X}^2_{[\mathbf{0},\mathbf{1}]})\mathbf{X}^2_{[\mathbf{2},\mathbf{1}]}$	$A_1^{*\oplus 3} \oplus \mathbf{Z}/2\mathbf{Z}$
25	2	A_6	$(\mathbf{A}^7)\mathbf{ABCBC}$	$\Lambda_{(25)}$
26		D_6	$(\mathbf{A}^6\mathbf{BC})\mathbf{A}^2\mathbf{BC}$	$A_1^{*\oplus 2}$
27		E_6	$(\mathbf{A}^5\mathbf{BC}^2)\mathbf{X}_{[\mathbf{3},\mathbf{1}]}\mathbf{A}^3$	A_2^*
28		$A_5 \oplus A_1$	$(\mathbf{A}^6)(\mathbf{A}^2)\mathbf{BCBC}$	$A_2^* \oplus \mathbf{Z}/2\mathbf{Z}$
29		$A_5 \oplus A_1$	$(\mathbf{A}^6)(\mathbf{A}^2)\mathbf{A}\mathbf{X}_{[\mathbf{2},-\mathbf{1}]}\mathbf{X}_{[\mathbf{1},-\mathbf{2}]}\mathbf{C}$	$A_1^* \oplus \langle 1/6 \rangle$
30		$D_5 \oplus A_1$	$(\mathbf{A}^5\mathbf{BC})(\mathbf{A}^2)\mathbf{ABC}$	$A_1^* \oplus \langle 1/4 \rangle$

No.	r	T	branes	$E(K)$
31	2	$A_4 \oplus A_2$	$(\mathbf{A}^5)(\mathbf{A}^3)\mathbf{BCBC}$	$\Lambda_{(31)}$
32		$D_4 \oplus A_2$	$(\mathbf{A}^4\mathbf{BC})(\mathbf{A}^3)\mathbf{ABC}$	$\Lambda_{(23)}$
33		$A_4 \oplus {A_1}^{\oplus 2}$	$(\mathbf{A}^5)(\mathbf{A}^2)^2\mathbf{X}_{[\mathbf{2},-\mathbf{1}]}\mathbf{X}_{[\mathbf{1},-\mathbf{2}]}\mathbf{C}$	$\Lambda_{(33)}$
34		$D_4 \oplus {A_1}^{\oplus 2}$	$(\mathbf{A}^4\mathbf{BC})(\mathbf{A}^2)^2\mathbf{BC}$	$A_1^{*\oplus 2} \oplus \mathbf{Z}/2\mathbf{Z}$
35		$A_3 \oplus A_3$	$(\mathbf{A}^4)^2\mathbf{BCBC}$	$A_1^{*\oplus 2} \oplus \mathbf{Z}/2\mathbf{Z}$
36		$A_3 \oplus A_3$	$(\mathbf{A}^4)^2\mathbf{A}\mathbf{X}_{[\mathbf{2},-\mathbf{1}]}\mathbf{X}_{[\mathbf{1},-\mathbf{2}]}\mathbf{C}$	$\langle 1/4\rangle^{\oplus 2}$
37		$A_3 \oplus A_2 \oplus A_1$	$(\mathbf{A}^4)(\mathbf{A}^3)(\mathbf{B}^2)\mathbf{X}_{[\mathbf{1},-\mathbf{3}]}\mathbf{CA}$	$A_1^* \oplus \langle 1/12\rangle$
38		$A_3 \oplus {A_1}^{\oplus 3}$	$(\mathbf{A}^4)(\mathbf{A}^2)(\mathbf{B}^2)(\mathbf{X}^2_{[\mathbf{0},\mathbf{1}]})\mathbf{BC}$	$A_1^* \oplus \langle 1/4\rangle \oplus \mathbf{Z}/2\mathbf{Z}$
39		${A_2}^{\oplus 3}$	$(\mathbf{A}^3)^3\mathbf{X}_{[\mathbf{2},-\mathbf{1}]}\mathbf{X}_{[\mathbf{1},-\mathbf{2}]}\mathbf{C}$	$A_2^* \oplus \mathbf{Z}/3\mathbf{Z}$
40		${A_2}^{\oplus 2} \oplus {A_1}^{\oplus 2}$	$(\mathbf{A}^3)^2(\mathbf{B}^2)(\mathbf{X}^2_{[\mathbf{0},\mathbf{1}]})\mathbf{BC}$	$\langle 1/6\rangle^{\oplus 2}$
41		$A_2 \oplus {A_1}^{\oplus 4}$	$(\mathbf{A}^3)(\mathbf{B}^2)(\mathbf{X}^2_{[\mathbf{0},\mathbf{1}]})(\mathbf{B}^2)(\mathbf{X}^2_{[\mathbf{0},\mathbf{1}]})\mathbf{A}$	$\Lambda_{(23)} \oplus \mathbf{Z}/2\mathbf{Z}$
42		${A_1}^{\oplus 6}$	$(\mathbf{A}^2)^2(\mathbf{B}^2)^2(\mathbf{X}^2_{[\mathbf{0},\mathbf{1}]})(\mathbf{X}^2_{[\mathbf{2},\mathbf{1}]})$	$A_1^{*\oplus 2} \oplus (\mathbf{Z}/2\mathbf{Z})^2$
43	1	E_7	$(\mathbf{A}^6\mathbf{BC}^2)\mathbf{X}_{[\mathbf{3},\mathbf{1}]}\mathbf{A}^2$	A_1^*
44		A_7	$(\mathbf{A}^8)\mathbf{BCBC}$	$A_1^* \oplus \mathbf{Z}/2\mathbf{Z}$
45		A_7	$(\mathbf{A}^8)\mathbf{A}\mathbf{X}_{[\mathbf{2},-\mathbf{1}]}\mathbf{X}_{[\mathbf{1},-\mathbf{2}]}\mathbf{C}$	$\langle 1/8\rangle$
46		D_7	$(\mathbf{A}^7\mathbf{BC})\mathbf{ABC}$	$\langle 1/4\rangle$
47		$A_6 \oplus A_1$	$(\mathbf{A}^7)(\mathbf{B}^2)\mathbf{X}_{[\mathbf{1},-\mathbf{3}]}\mathbf{CA}$	$\langle 1/14\rangle$
48		$D_6 \oplus A_1$	$(\mathbf{A}^6\mathbf{BC})(\mathbf{A}^2)\mathbf{BC}$	$A_1^* \oplus \mathbf{Z}/2\mathbf{Z}$
49		$E_6 \oplus A_1$	$(\mathbf{A}^2)(\mathbf{A}^5\mathbf{BC}^2)\mathbf{X}_{[\mathbf{3},\mathbf{1}]}\mathbf{A}$	$\langle 1/6\rangle$
50		$D_5 \oplus A_2$	$(\mathbf{A}^5\mathbf{BC})(\mathbf{A}^3)\mathbf{BC}$	$\langle 1/12\rangle$
51		$A_5 \oplus A_2$	$(\mathbf{A}^6)(\mathbf{A}^3)\mathbf{X}_{[\mathbf{2},-\mathbf{1}]}\mathbf{X}_{[\mathbf{1},-\mathbf{2}]}\mathbf{C}$	$A_1^* \oplus \mathbf{Z}/3\mathbf{Z}$
52		$D_5 \oplus {A_1}^{\oplus 2}$	$(\mathbf{A}^5\mathbf{BC})(\mathbf{B}^2)(\mathbf{X}^2_{[\mathbf{0},\mathbf{1}]})\mathbf{A}$	$\langle 1/4\rangle \oplus \mathbf{Z}/2\mathbf{Z}$
53		$A_5 \oplus {A_1}^{\oplus 2}$	$(\mathbf{A}^6)(\mathbf{B}^2)(\mathbf{X}^2_{[\mathbf{0},\mathbf{1}]})\mathbf{BC}$	$\langle 1/6\rangle \oplus \mathbf{Z}/2\mathbf{Z}$
54		$D_4 \oplus A_3$	$(\mathbf{A}^4\mathbf{BC})(\mathbf{A}^4)\mathbf{BC}$	$\langle 1/4\rangle \oplus \mathbf{Z}/2\mathbf{Z}$
55		$A_4 \oplus A_3$	$(\mathbf{A}^5)(\mathbf{A}^4)\mathbf{X}_{[\mathbf{2},-\mathbf{1}]}\mathbf{X}_{[\mathbf{1},-\mathbf{2}]}\mathbf{C}$	$\langle 1/20\rangle$
56		$A_4 \oplus A_2 \oplus A_1$	$(\mathbf{A}^5)(\mathbf{A}^3)(\mathbf{B}^2)\mathbf{X}_{[\mathbf{1},-\mathbf{3}]}\mathbf{C}$	$\langle 1/30\rangle$
57		$D_4 \oplus {A_1}^{\oplus 3}$	$(\mathbf{A}^4\mathbf{BC})(\mathbf{A}^2)(\mathbf{B}^2)(\mathbf{X}^2_{[\mathbf{0},\mathbf{1}]})$	$A_1^* \oplus (\mathbf{Z}/2\mathbf{Z})^2$
58		${A_3}^{\oplus 2} \oplus A_1$	$(\mathbf{A}^4)^2(\mathbf{B}^2)\mathbf{X}_{[\mathbf{1},-\mathbf{3}]}\mathbf{C}$	$A_1^* \oplus \mathbf{Z}/4\mathbf{Z}$
59		$A_3 \oplus A_2 \oplus {A_1}^{\oplus 2}$	$(\mathbf{A}^4)(\mathbf{B}^3)(\mathbf{X}^2_{[\mathbf{0},\mathbf{1}]})(\mathbf{X}^2_{[\mathbf{2},\mathbf{1}]})\mathbf{X}_{[\mathbf{3},\mathbf{1}]}$	$\langle 1/12\rangle \oplus \mathbf{Z}/2\mathbf{Z}$
60		$A_3 \oplus {A_1}^{\oplus 4}$	$(\mathbf{A}^4)(\mathbf{B}^2)(\mathbf{X}^2_{[\mathbf{0},\mathbf{1}]})(\mathbf{B}^2)(\mathbf{X}^2_{[\mathbf{0},\mathbf{1}]})$	$\langle 1/4\rangle \oplus (\mathbf{Z}/2\mathbf{Z})^2$
61		${A_2}^{\oplus 3} \oplus A_1$	$(\mathbf{A}^3)^2(\mathbf{B}^3)(\mathbf{X}^2_{[\mathbf{1},-\mathbf{2}]})\mathbf{C}$	$\langle 1/6\rangle \oplus \mathbf{Z}/3\mathbf{Z}$

No.	r	T	branes	$E(K)$
62	0	E_8	$(\mathbf{A}^7\mathbf{B}\mathbf{C}^2)\mathbf{X}_{[\mathbf{3},\mathbf{1}]}\mathbf{A}$	0
63		A_8	$(\mathbf{A}^9)\mathbf{X}_{[\mathbf{2},-\mathbf{1}]}\mathbf{X}_{[\mathbf{1},-\mathbf{2}]}\mathbf{C}$	$\mathbf{Z}/3\mathbf{Z}$
64		D_8	$(\mathbf{A}^8\mathbf{B}\mathbf{C})\mathbf{B}\mathbf{C}$	$\mathbf{Z}/2\mathbf{Z}$
65		$E_7 \oplus A_1$	$(\mathbf{A}^2)(\mathbf{A}^6\mathbf{B}\mathbf{C}^2)\mathbf{X}_{[\mathbf{3},\mathbf{1}]}$	$\mathbf{Z}/2\mathbf{Z}$
66		$A_5 \oplus A_2 \oplus A_1$	$(\mathbf{A}^6)(\mathbf{B}^3)(\mathbf{X}^2_{[\mathbf{1},-\mathbf{2}]})\mathbf{C}$	$\mathbf{Z}/6\mathbf{Z}$
67		${A_4}^{\oplus 2}$	$(\mathbf{A}^5)(\mathbf{B}^5)\mathbf{X}_{[\mathbf{2},-\mathbf{3}]}\mathbf{C}$	$\mathbf{Z}/5\mathbf{Z}$
68		${A_2}^{\oplus 4}$	$(\mathbf{A}^3)(\mathbf{B}^3)(\mathbf{X}^3_{[\mathbf{0},\mathbf{1}]})(\mathbf{C}^3)$	$(\mathbf{Z}/3\mathbf{Z})^2$
69		$E_6 \oplus A_2$	$(\mathbf{A}^3)(\mathbf{A}^5\mathbf{B}\mathbf{C}^2)\mathbf{X}_{[\mathbf{3},\mathbf{1}]}$	$\mathbf{Z}/3\mathbf{Z}$
70		$A_7 \oplus A_1$	$(\mathbf{A}^8)(\mathbf{B}^2)\mathbf{X}_{[\mathbf{1},-\mathbf{3}]}\mathbf{C}$	$\mathbf{Z}/4\mathbf{Z}$
71		$D_6 \oplus {A_1}^{\oplus 2}$	$(\mathbf{A}^6\mathbf{B}\mathbf{C})(\mathbf{B}^2)(\mathbf{X}^2_{[\mathbf{0},\mathbf{1}]})$	$(\mathbf{Z}/2\mathbf{Z})^2$
72		$D_5 \oplus A_3$	$(\mathbf{A}^5\mathbf{B}\mathbf{C})(\mathbf{B}^4)\mathbf{X}_{[\mathbf{1},-\mathbf{2}]}$	$\mathbf{Z}/4\mathbf{Z}$
73		${D_4}^{\oplus 2}$	$(\mathbf{A}^4\mathbf{B}\mathbf{C})(\mathbf{A}^4\mathbf{B}\mathbf{C})$	$(\mathbf{Z}/2\mathbf{Z})^2$
74		$(A_3 \oplus A_1)^{\oplus 2}$	$(\mathbf{A}^4)(\mathbf{B}^4)(\mathbf{X}^2_{[\mathbf{0},\mathbf{1}]})(\mathbf{X}^2_{[\mathbf{2},\mathbf{1}]})$	$\mathbf{Z}/4\mathbf{Z} \oplus \mathbf{Z}/2\mathbf{Z}$

Table 2: Brane configurations

where

$$\begin{aligned} &\text{(a)} \quad \mathbf{z}'_i = \mathbf{z}_{i+1}, \quad \mathbf{z}'_{i+1} = \mathbf{z}_i + (\mathbf{z}_i \times \mathbf{z}_{i+1})\,\mathbf{z}_{i+1}, \\ &\text{(b)} \quad \mathbf{z}'_i = \mathbf{z}_{i+1} + (\mathbf{z}_i \times \mathbf{z}_{i+1})\,\mathbf{z}_i, \quad \mathbf{z}'_{i+1} = \mathbf{z}_i \end{aligned} \tag{3.22}$$

with $\mathbf{z}_i \times \mathbf{z}_j = p_i q_j - p_j q_i$ for $\mathbf{z}_i = (p_i, q_i)$. Under the brane move (3.21), the charges Q_i also change as

$$\begin{aligned} &\text{(a)} \quad Q'_i = Q_{i+1} - (\mathbf{z}_i \times \mathbf{z}_{i+1})Q_i, \quad Q'_{i+1} = Q_i, \\ &\text{(b)} \quad Q'_i = Q_{i+1}, \quad Q'_{i+1} = Q_i - (\mathbf{z}_i \times \mathbf{z}_{i+1})Q_{i+1}, \end{aligned} \tag{3.23}$$

in such a way that

$$Q_i \mathbf{z}_i + Q_{i+1}\mathbf{z}_{i+1} = Q'_i \mathbf{z}'_i + Q'_{i+1}\mathbf{z}'_{i+1}, \tag{3.24}$$

thereby the total charges are kept invariant. Moreover, what is important is that the brane moves preserve the junction lattice. That is, under the unimodular transformation (3.23) we can prove the relation

$$-\mathbf{J}^2 = \sum_{i,j} Q_i(\mathbf{s}_i, \mathbf{s}_j)Q_j = \sum_{i,j} Q'_i(\mathbf{s}'_i, \mathbf{s}'_j)Q'_j = -\mathbf{J}'^2. \tag{3.25}$$

To this end, let us rewrite $\mathbf{J}^2$ as

$$-\mathbf{J}^2 = \sum_i Q_i \bar{Q}_i, \qquad \bar{Q}_i = Q_i - \sum_{k<i} (\mathbf{z}_k \times \mathbf{z}_i) Q_k. \tag{3.26}$$

Then, invariance of $\mathbf{J}^2$ follows from the transformation formulae for $\bar{Q}_j$ given by

$$\begin{aligned} &\text{(a)} \quad \bar{Q}'_i = \bar{Q}_{i+1}, \quad \bar{Q}'_{i+1} = \bar{Q}_i + (\mathbf{z}_i \times \mathbf{z}_{i+1}) \bar{Q}_{i+1}, \\ &\text{(b)} \quad \bar{Q}'_i = \bar{Q}_{i+1} + (\mathbf{z}_i \times \mathbf{z}_{i+1}) \bar{Q}_i, \quad \bar{Q}'_{i+1} = \bar{Q}_i. \end{aligned} \tag{3.27}$$

Now we find brane configurations for every T as shown in Table 2 where the branes put in the parenthesis are the mutually coinciding ones corresponding to the singular fibers. We note that the $\mathbf{A_n}$ branes are used to represent the A_n singularity with $n = 0, 1, 2$, though one may use $\mathbf{H_n}$ as well without changing the structure of $E(K)$. All the configurations in Table 2 can be obtained from the $\widehat{\mathbf{E}}_9$ configuration (3.10) by suitable brane moves. This means that the lattice T in Table 2 can be realized as a sub-lattice of the junction lattice on $\widehat{\mathbf{E}}_9$, hence $T \subset E_8$.

Example. (No.63)

The move from $\mathbf{A}^8\mathbf{BCBC}$ to $\mathbf{A}^9\mathbf{X}_{[\mathbf{2},-\mathbf{1}]}\mathbf{X}_{[\mathbf{1},-\mathbf{2}]}\mathbf{C}$ is given as follows:

$$\begin{aligned} \mathbf{A}^8\mathbf{BCBC} &= \mathbf{A}^8\mathbf{BC}^2\mathbf{X}_{[\mathbf{3},\mathbf{1}]} = \mathbf{A}^7\mathbf{BX}_{[\mathbf{0},\mathbf{1}]}\mathbf{C}^2\mathbf{X}_{[\mathbf{3},\mathbf{1}]} = \mathbf{A}^7\mathbf{BA}^2\mathbf{X}_{[\mathbf{0},\mathbf{1}]}\mathbf{X}_{[\mathbf{3},\mathbf{1}]} \\ &= \mathbf{A}^9\mathbf{X}_{[\mathbf{3},-\mathbf{1}]}\mathbf{X}_{[\mathbf{0},\mathbf{1}]}\mathbf{X}_{[\mathbf{3},\mathbf{1}]} = \mathbf{A}^8\mathbf{X}_{[\mathbf{2},-\mathbf{1}]}\mathbf{CX}_{[\mathbf{4},\mathbf{1}]}\mathbf{A} \\ &= \mathbf{A}^8\mathbf{X}_{[\mathbf{2},-\mathbf{1}]}\mathbf{X}_{[\mathbf{1},-\mathbf{2}]}\mathbf{CA} = \mathbf{A}^9\mathbf{X}_{[\mathbf{2},-\mathbf{1}]}\mathbf{X}_{[\mathbf{1},-\mathbf{2}]}\mathbf{C}. \end{aligned} \tag{3.28}$$

It is also possible to find corresponding curves. Some of them have already been given in section 2, from which it is clear how to identify a curve with an entry of Table 2. Let us enumerate more examples based on [18, 1, 2]. The massive $\widehat{E}_n$ $(n = 8, ..., 1)$ and $\widehat{\widehat{E}}_1$ curves correspond to Nos. 1, 2, 3, 5, 8, 15, 25, 44 and 45, respectively. The massless $\widehat{E}_n$ $(n = 8, ..., 3, 1)$ and $\widehat{\widehat{E}}_0$ curves correspond to Nos. 62, 65, 69, 72, 67, 66, 70 and 63, respectively. The Seiberg-Witten curves for $\mathcal{N} = 2$ $SU(2)$ theory with various flavor symmetries [15] can be identified with No.64 ($N_f = 0$), No.46 ($N_f = 1$), Nos. 26, 48, 71 ($N_f = 2$), Nos. 16, 30, 50, 52, 72 ($N_f = 3$) and Nos. 9, 18, 32, 34, 54, 57, 73 ($N_f = 4$). In each case, the number of independent mass parameters is given by $r = \operatorname{rank} E(K)$. For the extremal cases $r = 0$, the curves and sections were explicitly obtained earlier in [22].

When we consider curves in view of Table 2 there is a point to notice. As remarked above, one can use either $\mathbf{A_n}$ or $\mathbf{H_n}$ branes to describe the A_n singular fibers with $n = 0, 1, 2$. This does not change the structure of $E(K)$, whereas it does change the explicit form of corresponding elliptic curves, and hence we are led to different physical interpretation. To clarify the point, let us examine the case of $E(K) = E_8$, E_7^*, E_6^*. The 7-branes are rewritten as

$$(\mathbf{A}^{9-N})\mathbf{A}^{N-1}\mathbf{BCBC} = (\mathbf{A}^{9-N})\mathbf{X}_{[\mathbf{N-6},\mathbf{1}]}\mathbf{A}^{N-1}\mathbf{BC}^2 \tag{3.29}$$

for $N = 8, 7, 6$. Since the configuration $(\mathbf{A}^{9-N})\mathbf{X}_{[\mathbf{N-6},\mathbf{1}]}$ is equivalent to $(\mathbf{A}^{9-N})\mathbf{C}$ up to $SL(2, \mathbf{Z})$ conjugation, further coalescence can occur

$$(\mathbf{A}^{9-N})\mathbf{X}_{[\mathbf{N-6},\mathbf{1}]} \longrightarrow (\mathbf{A}^{9-N}\mathbf{X}_{[\mathbf{N-6},\mathbf{1}]}) = \mathbf{H}_{\mathbf{N-1}}, \tag{3.30}$$

which also yields $T = A_{8-N}$. Although the singularity structure of T is identical, it is shown in [1] that the limit (3.30) gives rise to the compactification of 5D $\mathcal{N} = 1$ E_N theories down to 4D $\mathcal{N} = 2$ E_N theories for $N = 8, 7, 6$. Thus the structure of $E(K)$ seems not sensitive enough to distinguish these two theories.

In solving the problem (2), we recognize that the global structure of the surface S plays a relevant role in determining the lattice L. This point is now illuminated by working out several examples.

3.3.1 Case of Cartan type

Let us first consider the case No.7 using the brane configuration $(\mathbf{A}^2)^3\mathbf{A}^2\mathbf{BCBC}$. Accordingly, we put $\mathbf{s}_i = \mathbf{a}_i$ $(1 \leq i \leq 8)$, $\mathbf{s}_9 = \mathbf{b}_1$, $\mathbf{s}_{10} = \mathbf{c}_1$, $\mathbf{s}_{11} = \mathbf{b}_2$ and $\mathbf{s}_{12} = \mathbf{c}_2$, where $\mathbf{a}$, $\mathbf{b}$ and $\mathbf{c}$ denote outgoing $(1, 0)$-, $(1, -1)$- and $(1, 1)$-strings attached to $\mathbf{A}$, $\mathbf{B}$ and $\mathbf{C}$ branes, respectively. (Notice that the assignment of $\mathbf{s}_j$ may be different from this for other cases depending on the brane configuration.) Choose the root junctions generating the lattice $T = {A_1}^{\oplus 3}$ as

$$\boldsymbol{\alpha}_1 = \mathbf{s}_1 - \mathbf{s}_2, \qquad \boldsymbol{\alpha}_2 = \mathbf{s}_3 - \mathbf{s}_4, \qquad \boldsymbol{\alpha}_3 = \mathbf{s}_5 - \mathbf{s}_6. \tag{3.31}$$

These junctions are supported by the collapsible branes $\mathbf{A}_1\mathbf{A}_2$, $\mathbf{A}_3\mathbf{A}_4$ and $\mathbf{A}_5\mathbf{A}_6$, respectively, and there remain 6 branes $\mathbf{A}^2\mathbf{BCBC}$ of $\widehat{\mathbf{E}}_\mathbf{9}$. From Table 2 we see that the

corresponding Mordell-Weil lattice is $E(K) = L^* = D_4^* \oplus A_1^*$. These lattices are canonically realized on the 7-branes $\mathbf{A}^4\mathbf{BC}$ and $\mathbf{A}^2$. Thus one needs apparently 8 branes, which is more than the remaining ones. This puzzle, however, can be resolved if we consider junctions containing strings which encircle the branes supporting T. To do so, we note that the general form of junctions which are orthogonal to T with $(p, q) = (0, 0)$ is parameterized as

$$\begin{aligned}\mathbf{j} = & Q_1(\mathbf{s}_1 + \mathbf{s}_2) + Q_3(\mathbf{s}_3 + \mathbf{s}_4) + Q_5(\mathbf{s}_5 + \mathbf{s}_6) \\ & -(2Q_1 + 2Q_3 + 2Q_5 + Q_8 + 2Q_{10} + 2Q_{12})\mathbf{s}_7 + Q_8\mathbf{s}_8 \\ & +(Q_{10} - Q_{11} + Q_{12})\mathbf{s}_9 + Q_{10}\mathbf{s}_{10} + Q_{11}\mathbf{s}_{11} + Q_{12}\mathbf{s}_{12}. \end{aligned} \tag{3.32}$$

Thus these junctions span the 7-dimensional lattice. This junction lattice has elements along the null junctions (3.18) and the remaining ones form a lattice of rank 5, which is expected to be isomorphic to the lattice $D_4 \oplus A_1$. In fact one can find the generators of $L = D_4 \oplus A_1$ as

$$\begin{aligned}\mathbf{j}_1 &= \mathbf{s}_7 + \mathbf{s}_8 - \mathbf{s}_9 - \mathbf{s}_{10}, \\ \mathbf{j}_2 &= -\mathbf{s}_9 + \mathbf{s}_{11}, \\ \mathbf{j}_3 &= \mathbf{s}_5 + \mathbf{s}_6 - \mathbf{s}_9 - \mathbf{s}_{10}, \\ \mathbf{j}_4 &= \mathbf{s}_3 + \mathbf{s}_4 - \mathbf{s}_9 - \mathbf{s}_{10}, \\ \mathbf{j}_5 &= \mathbf{s}_7 - \mathbf{s}_8, \end{aligned} \tag{3.33}$$

where $\mathbf{j}_i$ with $1 \leq i \leq 4$ are for D_4 and $\mathbf{j}_5$ is for A_1. Some of the strings in these junctions are ending on the 7-branes which support the lattice T generated by (3.31). It is observed, however, that they take the form of tadpole loops of (3.13) locally around each of the collapsible branes $\mathbf{A}_1\mathbf{A}_2$, $\mathbf{A}_3\mathbf{A}_4$ and $\mathbf{A}_5\mathbf{A}_6$ (see Figure 3), and hence the generators (3.33) are in fact orthogonal to T. It should be noted that any junction orthogonal to the lattice T in Table 2 is of the form of (3.13)–(3.15) locally around the coinciding $\mathbf{A_n}$, $\mathbf{D_n}$ and $\mathbf{E_n}$ branes which describe the singular fibers.

In a similar manner we construct the basis junctions of L for the other cases of Cartan type intersections. The results are presented in Tables 3–7 where $C(\mathcal{G})$ denotes the Cartan matrix of the Lie algebra $\mathcal{G}$ and the self-intersection (times (-1)) of the i-th junction is given by the (i, i) element of the intersection matrix in the third column.

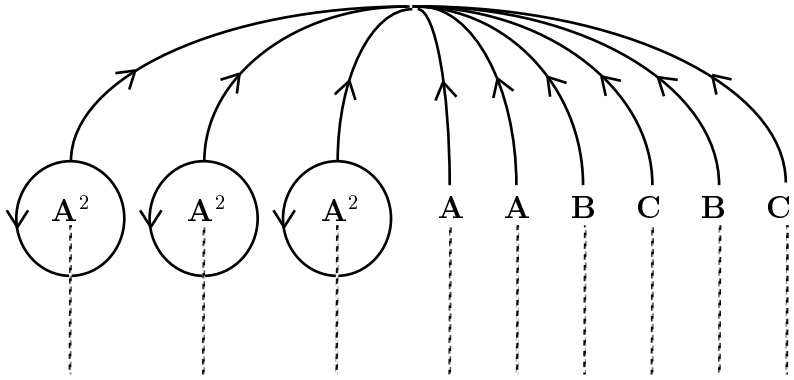

Figure 3: Junctions orthogonal to T.

No.	basis	$-(\mathbf{j},\mathbf{j})$
1	$\mathbf{s}_2-\mathbf{s}_3,\quad \mathbf{s}_3-\mathbf{s}_4,\quad \mathbf{s}_4-\mathbf{s}_5,\quad \mathbf{s}_5-\mathbf{s}_6,\quad \mathbf{s}_6-\mathbf{s}_7,$ $\mathbf{s}_7+\mathbf{s}_8-\mathbf{s}_{11}-\mathbf{s}_{12},\quad \mathbf{s}_{10}-\mathbf{s}_{12},\quad \mathbf{s}_7-\mathbf{s}_8$	$C(E_8)$
2	$\mathbf{s}_3-\mathbf{s}_4,\quad \mathbf{s}_4-\mathbf{s}_5,\quad \mathbf{s}_5-\mathbf{s}_6,\quad \mathbf{s}_6-\mathbf{s}_7,$ $\mathbf{s}_7+\mathbf{s}_8-\mathbf{s}_{11}-\mathbf{s}_{12},\quad \mathbf{s}_{10}-\mathbf{s}_{12},\quad \mathbf{s}_7-\mathbf{s}_8$	$C(E_7)$
3	$\mathbf{s}_3-\mathbf{s}_4,\quad \mathbf{s}_4-\mathbf{s}_5,\quad \mathbf{s}_5-\mathbf{s}_6,\quad \mathbf{s}_6-\mathbf{s}_7,$ $\mathbf{s}_7+\mathbf{s}_8-\mathbf{s}_{11}-\mathbf{s}_{12},\quad \mathbf{s}_{10}-\mathbf{s}_{12},\quad \mathbf{s}_7-\mathbf{s}_8$	$C(E_6)$
4	$\mathbf{s}_{10}-\mathbf{s}_{12},\quad -\mathbf{s}_3-\mathbf{s}_4-\mathbf{s}_{10}+\mathbf{s}_{11}+\mathbf{s}_{12},$ $\mathbf{s}_3+\mathbf{s}_4+\mathbf{s}_7+\mathbf{s}_8+\mathbf{s}_{10}-2\mathbf{s}_{11}-3\mathbf{s}_{12},$ $\mathbf{s}_6-\mathbf{s}_7,\quad \mathbf{s}_5-\mathbf{s}_6,\quad \mathbf{s}_7-\mathbf{s}_8$	$C(D_6)$
5	$\mathbf{s}_{10}-\mathbf{s}_{12},\quad \mathbf{s}_7+\mathbf{s}_8-\mathbf{s}_9-\mathbf{s}_{10},$ $\mathbf{s}_6-\mathbf{s}_7,\quad \mathbf{s}_5-\mathbf{s}_6,\quad \mathbf{s}_7-\mathbf{s}_8$	$C(D_5)$
6	$\mathbf{s}_4+\mathbf{s}_5+\mathbf{s}_6+\mathbf{s}_7+\mathbf{s}_{10}-2\mathbf{s}_{11}-3\mathbf{s}_{12},$ $-\mathbf{s}_7+\mathbf{s}_8,\quad -\mathbf{s}_6+\mathbf{s}_7,$ $-\mathbf{s}_7-\mathbf{s}_8-\mathbf{s}_{10}+\mathbf{s}_{10}+2\mathbf{s}_{12},\quad \mathbf{s}_{10}-\mathbf{s}_{12}$	$C(A_5)$
7	$\mathbf{s}_7+\mathbf{s}_8-\mathbf{s}_9-\mathbf{s}_{10},$ $-\mathbf{s}_9+\mathbf{s}_{11},\quad \mathbf{s}_5+\mathbf{s}_6-\mathbf{s}_9-\mathbf{s}_{10},$ $\mathbf{s}_3+\mathbf{s}_4-\mathbf{s}_9-\mathbf{s}_{10},$ $\mathbf{s}_7-\mathbf{s}_8$	$\begin{pmatrix} 2 & -1 & 0 & 0 & 0 \\ -1 & 2 & -1 & -1 & 0 \\ 0 & -1 & 2 & 0 & 0 \\ 0 & -1 & 0 & 2 & 0 \\ 0 & 0 & 0 & 0 & 2 \end{pmatrix}$

Table 3: The basis junctions for $r \geq 5$.

No.	basis	$-(\mathbf{j},\mathbf{j})$
8	$\begin{cases} \mathbf{s}_{10}-\mathbf{s}_{12}, \\ \mathbf{s}_7+\mathbf{s}_8-\mathbf{s}_{11}-\mathbf{s}_{12}, \\ \mathbf{s}_6-\mathbf{s}_7, \\ \mathbf{s}_7-\mathbf{s}_8 \end{cases}$	$\begin{pmatrix} 2 & -1 & 0 & 0 \\ -1 & 2 & -1 & 0 \\ 0 & -1 & 2 & -1 \\ 0 & 0 & -1 & 2 \end{pmatrix}$
9	$\begin{cases} -\mathbf{s}_7+\mathbf{s}_8, \\ -\mathbf{s}_8+\mathbf{s}_9, \\ -\mathbf{s}_9+\mathbf{s}_{10}, \\ -\mathbf{s}_9-\mathbf{s}_{10}+\mathbf{s}_{11}+\mathbf{s}_{12} \end{cases}$	$\begin{pmatrix} 2 & -1 & 0 & 0 \\ -1 & 2 & -1 & -1 \\ 0 & -1 & 2 & 0 \\ 0 & -1 & 0 & 2 \end{pmatrix}$
10	$\begin{cases} -\mathbf{s}_7+\mathbf{s}_8, \\ -\mathbf{s}_7-\mathbf{s}_8+\mathbf{s}_{11}+\mathbf{s}_{12}, \\ -\mathbf{s}_{10}+\mathbf{s}_{12}, \\ -\mathbf{s}_5-\mathbf{s}_6+\mathbf{s}_{11}+\mathbf{s}_{12} \end{cases}$	$\begin{pmatrix} 2 & 0 & 0 & 0 \\ 0 & 2 & -1 & 0 \\ 0 & -1 & 2 & -1 \\ 0 & 0 & -1 & 2 \end{pmatrix}$
11	$\begin{cases} \mathbf{s}_4+\mathbf{s}_5+\mathbf{s}_6+\mathbf{s}_7+\mathbf{s}_{10}-2\mathbf{s}_{11}-3\mathbf{s}_{12}, \\ -\mathbf{s}_7+\mathbf{s}_8, \\ -\mathbf{s}_{10}+\mathbf{s}_{12}, \\ -\mathbf{s}_7-\mathbf{s}_8+\mathbf{s}_{11}+\mathbf{s}_{12} \end{cases}$	$\begin{pmatrix} 2 & -1 & 0 & 0 \\ -1 & 2 & 0 & 0 \\ 0 & 0 & 2 & -1 \\ 0 & 0 & -1 & 2 \end{pmatrix}$
12	$\begin{cases} \mathbf{s}_4+\mathbf{s}_5+2\mathbf{s}_8+\mathbf{s}_{10}-2\mathbf{s}_{11}-3\mathbf{s}_{12}, \\ \mathbf{s}_6+\mathbf{s}_7-\mathbf{s}_{11}-\mathbf{s}_{12}, \\ \mathbf{s}_{10}-\mathbf{s}_{12}, \\ \mathbf{s}_4+\mathbf{s}_5-\mathbf{s}_{11}-\mathbf{s}_{12} \end{cases}$	$\begin{pmatrix} 4 & -1 & 0 & 1 \\ -1 & 2 & -1 & 0 \\ 0 & -1 & 2 & -1 \\ 1 & 0 & -1 & 2 \end{pmatrix}$
13	$\begin{cases} -\mathbf{s}_7-\mathbf{s}_8+\mathbf{s}_{11}+\mathbf{s}_{12}, \\ -\mathbf{s}_{10}+\mathbf{s}_{12}, \\ -\mathbf{s}_3-\mathbf{s}_4+\mathbf{s}_{11}+\mathbf{s}_{12}, \\ -\mathbf{s}_5-\mathbf{s}_6+\mathbf{s}_{11}+\mathbf{s}_{12} \end{cases}$	$\begin{pmatrix} 2 & -1 & 0 & 0 \\ -1 & 2 & -1 & -1 \\ 0 & -1 & 2 & 0 \\ 0 & -1 & 0 & 2 \end{pmatrix}$
14	$\begin{cases} \mathbf{s}_3+\mathbf{s}_4+\mathbf{s}_9-\mathbf{s}_{11}-2\mathbf{s}_{12}, \\ \mathbf{s}_5+\mathbf{s}_6+\mathbf{s}_9-\mathbf{s}_{11}-2\mathbf{s}_{12}, \\ \mathbf{s}_7+\mathbf{s}_8+\mathbf{s}_9-\mathbf{s}_{11}-2\mathbf{s}_{12}, \\ \mathbf{s}_3+\mathbf{s}_4+\mathbf{s}_5+\mathbf{s}_6+\mathbf{s}_7+\mathbf{s}_8-2\mathbf{s}_{11}-4\mathbf{s}_{12} \end{cases}$	$\begin{pmatrix} 2 & 0 & 0 & 0 \\ 0 & 2 & 0 & 0 \\ 0 & 0 & 2 & 0 \\ 0 & 0 & 0 & 2 \end{pmatrix}$

Table 4: The basis junctions for $r = 4$.

No.	basis	$-(\mathbf{j},\mathbf{j})$
15	$\begin{cases} \mathbf{s}_7+\mathbf{s}_8+\mathbf{s}_{10}-\mathbf{s}_{11}-2\mathbf{s}_{12}, \\ -\mathbf{s}_{10}+\mathbf{s}_{12}, \\ \mathbf{s}_7-\mathbf{s}_8 \end{cases}$	$\begin{pmatrix} 2 & -1 & 0 \\ -1 & 2 & 0 \\ 0 & 0 & 2 \end{pmatrix}$
16	$\begin{cases} \mathbf{s}_8-\mathbf{s}_9, \\ -\mathbf{s}_8+\mathbf{s}_{10}, \\ \mathbf{s}_8+\mathbf{s}_9-\mathbf{s}_{11}-\mathbf{s}_{12} \end{cases}$	$\begin{pmatrix} 2 & -1 & 0 \\ -1 & 2 & -1 \\ 0 & -1 & 2 \end{pmatrix}$
17	$\begin{cases} 2\mathbf{s}_8+\mathbf{s}_{10}-\mathbf{s}_{11}-2\mathbf{s}_{12}, \\ \mathbf{s}_6+\mathbf{s}_7-\mathbf{s}_{11}-\mathbf{s}_{12}, \\ \mathbf{s}_{10}-\mathbf{s}_{12} \end{cases}$	$\begin{pmatrix} 4 & -1 & 1 \\ -1 & 2 & -1 \\ 1 & -1 & 2 \end{pmatrix}$
18	$\begin{cases} \mathbf{s}_9-\mathbf{s}_{10}, \\ \mathbf{s}_7+\mathbf{s}_8-\mathbf{s}_{11}-\mathbf{s}_{12}, \\ \mathbf{s}_9+\mathbf{s}_{10}-\mathbf{s}_{11}-\mathbf{s}_{12} \end{cases}$	$\begin{pmatrix} 2 & 0 & 0 \\ 0 & 2 & 0 \\ 0 & 0 & 2 \end{pmatrix}$
19	$\begin{cases} \mathbf{s}_5+\mathbf{s}_6+\mathbf{s}_7+\mathbf{s}_8+\mathbf{s}_{10}-2\mathbf{s}_{11}-3\mathbf{s}_{12}, \\ \mathbf{s}_{10}-\mathbf{s}_{12}, \\ -2\mathbf{s}_8-\mathbf{s}_{10}+\mathbf{s}_{11}+2\mathbf{s}_{12} \end{cases}$	$\begin{pmatrix} 2 & 0 & -1 \\ 0 & 2 & -1 \\ -1 & -1 & 4 \end{pmatrix}$
20	$\begin{cases} \mathbf{s}_{10}-\mathbf{s}_{12}, \\ \mathbf{s}_7+\mathbf{s}_8-\mathbf{s}_{11}-\mathbf{s}_{12}, \\ 2\mathbf{s}_4+2\mathbf{s}_5+2\mathbf{s}_6+\mathbf{s}_7+\mathbf{s}_8+2\mathbf{s}_{10}-4\mathbf{s}_{11}-6\mathbf{s}_{12} \end{cases}$	$\begin{pmatrix} 2 & -1 & 0 \\ -1 & 2 & 0 \\ 0 & 0 & 6 \end{pmatrix}$
21	$\begin{cases} \mathbf{s}_{10}-\mathbf{s}_{12}, \\ \mathbf{s}_5+\mathbf{s}_6-\mathbf{s}_{11}-\mathbf{s}_{12}, \\ -\mathbf{s}_5-\mathbf{s}_6-\mathbf{s}_7-\mathbf{s}_8-\mathbf{s}_{10}+2\mathbf{s}_{11}+3\mathbf{s}_{12} \end{cases}$	$\begin{pmatrix} 2 & -1 & 0 \\ -1 & 2 & -1 \\ 0 & -1 & 2 \end{pmatrix}$
22	$\begin{cases} \mathbf{s}_5+\mathbf{s}_6+\mathbf{s}_9-\mathbf{s}_{11}-2\mathbf{s}_{12}, \\ \mathbf{s}_7+\mathbf{s}_8+\mathbf{s}_9-\mathbf{s}_{11}-2\mathbf{s}_{12}, \\ \mathbf{s}_5+\mathbf{s}_6+\mathbf{s}_7+\mathbf{s}_8-\mathbf{s}_9-\mathbf{s}_{11}-2\mathbf{s}_{12} \end{cases}$	$\begin{pmatrix} 2 & 0 & 0 \\ 0 & 2 & 0 \\ 0 & 0 & 4 \end{pmatrix}$
23	$\begin{cases} \mathbf{s}_4+\mathbf{s}_5+\mathbf{s}_6+\mathbf{s}_7+\mathbf{s}_8+\mathbf{s}_9-2\mathbf{s}_{11}-4\mathbf{s}_{12}, \\ -\mathbf{s}_4-\mathbf{s}_5+\mathbf{s}_6+\mathbf{s}_7, \\ \mathbf{s}_4+\mathbf{s}_5-\mathbf{s}_8-\mathbf{s}_9 \end{cases}$	$\begin{pmatrix} 2 & 0 & 0 \\ 0 & 4 & -2 \\ 0 & -2 & 4 \end{pmatrix}$
24	$\begin{cases} \mathbf{s}_3+\mathbf{s}_4-\mathbf{s}_7-\mathbf{s}_8-\mathbf{s}_9-\mathbf{s}_{10}, \\ \mathbf{s}_3+\mathbf{s}_4+\mathbf{s}_7+\mathbf{s}_8+2\mathbf{s}_9+2\mathbf{s}_{10}-\mathbf{s}_{11}-\mathbf{s}_{12}, \\ \mathbf{s}_{11}-\mathbf{s}_{12} \end{cases}$	$\begin{pmatrix} 2 & 0 & 0 \\ 0 & 2 & 0 \\ 0 & 0 & 2 \end{pmatrix}$

Table 5: The basis junctions for $r = 3$.

No.	basis	$-(\mathbf{j},\mathbf{j})$
25	$-2\mathbf{s}_8+\mathbf{s}_{11}+\mathbf{s}_{12}$, $-\mathbf{s}_{10}+\mathbf{s}_{12}$	$\begin{pmatrix} 4 & -1 \\ -1 & 2 \end{pmatrix}$
26	$-\mathbf{s}_9-\mathbf{s}_{10}+\mathbf{s}_{11}+\mathbf{s}_{12}$, $-\mathbf{s}_9+\mathbf{s}_{10}$	$\begin{pmatrix} 2 & 0 \\ 0 & 2 \end{pmatrix}$
27	$-\mathbf{s}_{10}+\mathbf{s}_{11}$, $-\mathbf{s}_{11}+\mathbf{s}_{12}$	$\begin{pmatrix} 2 & -1 \\ -1 & 2 \end{pmatrix}$
28	$-\mathbf{s}_{10}+\mathbf{s}_{12}$, $-\mathbf{s}_7-\mathbf{s}_8+\mathbf{s}_{11}+\mathbf{s}_{12}$	$\begin{pmatrix} 2 & -1 \\ -1 & 2 \end{pmatrix}$
29	$-\mathbf{s}_7-\mathbf{s}_8-\mathbf{s}_9+\mathbf{s}_{11}+2\mathbf{s}_{12}$, $\mathbf{s}_7+\mathbf{s}_8-2\mathbf{s}_9$	$\begin{pmatrix} 2 & 0 \\ 0 & 6 \end{pmatrix}$
30	$-\mathbf{s}_8-\mathbf{s}_9+\mathbf{s}_{11}+\mathbf{s}_{12}$, $-2\mathbf{s}_{10}+\mathbf{s}_{11}+\mathbf{s}_{12}$	$\begin{pmatrix} 2 & 0 \\ 0 & 4 \end{pmatrix}$
31	$2\mathbf{s}_6+2\mathbf{s}_7+2\mathbf{s}_8+2\mathbf{s}_{10}-3\mathbf{s}_{11}-5\mathbf{s}_{12}$, $-\mathbf{s}_{10}+\mathbf{s}_{12}$	$\begin{pmatrix} 8 & -1 \\ -1 & 2 \end{pmatrix}$
32	$-\mathbf{s}_7-\mathbf{s}_8-\mathbf{s}_9+\mathbf{s}_{10}+\mathbf{s}_{11}+\mathbf{s}_{12}$, $-2\mathbf{s}_{10}+\mathbf{s}_{11}+\mathbf{s}_{12}$	$\begin{pmatrix} 4 & -2 \\ -2 & 4 \end{pmatrix}$
33	$-\mathbf{s}_6-\mathbf{s}_7-2\mathbf{s}_8-2\mathbf{s}_9+2\mathbf{s}_{11}+4\mathbf{s}_{12}$, $-\mathbf{s}_6-\mathbf{s}_7+\mathbf{s}_8+\mathbf{s}_9$	$\begin{pmatrix} 6 & -2 \\ -2 & 4 \end{pmatrix}$
34	$\mathbf{s}_9+\mathbf{s}_{10}-\mathbf{s}_{11}-\mathbf{s}_{12}$, $\mathbf{s}_7+\mathbf{s}_8-\mathbf{s}_{11}-\mathbf{s}_{12}$	$\begin{pmatrix} 2 & 0 \\ 0 & 2 \end{pmatrix}$
35	$-\mathbf{s}_5-\mathbf{s}_6-\mathbf{s}_7-\mathbf{s}_8-\mathbf{s}_{10}+2\mathbf{s}_{11}+3\mathbf{s}_{12}$, $-\mathbf{s}_{10}+\mathbf{s}_{12}$	$\begin{pmatrix} 2 & 0 \\ 0 & 2 \end{pmatrix}$
36	$-\mathbf{s}_5-\mathbf{s}_6-\mathbf{s}_7-\mathbf{s}_8+\mathbf{s}_9+\mathbf{s}_{11}+2\mathbf{s}_{12}$, $\mathbf{s}_5+\mathbf{s}_6+\mathbf{s}_7+\mathbf{s}_8+2\mathbf{s}_9-2\mathbf{s}_{11}-4\mathbf{s}_{12}$	$\begin{pmatrix} 4 & 0 \\ 0 & 4 \end{pmatrix}$
37	$-\mathbf{s}_5-\mathbf{s}_6-\mathbf{s}_7+\mathbf{s}_{10}+3\mathbf{s}_{11}-\mathbf{s}_{12}$, $\mathbf{s}_5+\mathbf{s}_6+\mathbf{s}_7-3\mathbf{s}_{12}$	$\begin{pmatrix} 2 & 0 \\ 0 & 12 \end{pmatrix}$

Table 6: The basis junctions for $r = 2$ (continued on Table 7).

No.	basis	$-(\mathbf{j},\mathbf{j})$
38	$-\mathbf{s}_5-\mathbf{s}_6+\mathbf{s}_{11}+\mathbf{s}_{12}$, $-\mathbf{s}_5-\mathbf{s}_6-\mathbf{s}_9-\mathbf{s}_{10}+2\mathbf{s}_{12}$	$\begin{pmatrix}2&0\\0&4\end{pmatrix}$
39	$\mathbf{s}_4+\mathbf{s}_5+\mathbf{s}_6-\mathbf{s}_{11}-2\mathbf{s}_{12}$, $\mathbf{s}_7+\mathbf{s}_8+\mathbf{s}_9-\mathbf{s}_{11}-2\mathbf{s}_{12}$	$\begin{pmatrix}2&-1\\-1&2\end{pmatrix}$
40	$-2\mathbf{s}_4-2\mathbf{s}_5-2\mathbf{s}_6-\mathbf{s}_9-\mathbf{s}_{10}+2\mathbf{s}_{11}+4\mathbf{s}_{12}$, $-\mathbf{s}_9-\mathbf{s}_{10}-\mathbf{s}_{11}+\mathbf{s}_{12}$	$\begin{pmatrix}6&0\\0&6\end{pmatrix}$
41	$\mathbf{s}_8+\mathbf{s}_9+\mathbf{s}_{10}+\mathbf{s}_{11}-2\mathbf{s}_{12}$, $-\mathbf{s}_6-\mathbf{s}_7+\mathbf{s}_{10}+\mathbf{s}_{11}$	$\begin{pmatrix}4&-2\\-2&4\end{pmatrix}$
42	$\mathbf{s}_3+\mathbf{s}_4+\mathbf{s}_7+\mathbf{s}_8+2\mathbf{s}_9+2\mathbf{s}_{10}-\mathbf{s}_{11}-\mathbf{s}_{12}$, $\mathbf{s}_3+\mathbf{s}_4-\mathbf{s}_7-\mathbf{s}_8-\mathbf{s}_9-\mathbf{s}_{10}$	$\begin{pmatrix}2&0\\0&2\end{pmatrix}$
43	$\mathbf{s}_{11}-\mathbf{s}_{12}$	2
44	$\mathbf{s}_{10}-\mathbf{s}_{12}$	2
45	$3\mathbf{s}_9-\mathbf{s}_{11}-2\mathbf{s}_{12}$	8
46	$2\mathbf{s}_{10}-\mathbf{s}_{11}-\mathbf{s}_{12}$	4
47	$\mathbf{s}_{10}+3\mathbf{s}_{11}-4\mathbf{s}_{12}$	14
48	$\mathbf{s}_9+\mathbf{s}_{10}-\mathbf{s}_{11}-\mathbf{s}_{12}$	2
49	$\mathbf{s}_3+\cdots+\mathbf{s}_7+2\mathbf{s}_9+2\mathbf{s}_{10}-4\mathbf{s}_{11}+3\mathbf{s}_{12}$	6
50	$2\mathbf{s}_8+2\mathbf{s}_9+2\mathbf{s}_{10}-3\mathbf{s}_{11}-3\mathbf{s}_{12}$	12
51	$\mathbf{s}_7+\mathbf{s}_8+\mathbf{s}_9-\mathbf{s}_{11}-2\mathbf{s}_{12}$	2
52	$\mathbf{s}_8+\mathbf{s}_9+\mathbf{s}_{10}-\mathbf{s}_{11}-2\mathbf{s}_{12}$	4
53	$\mathbf{s}_9+\mathbf{s}_{10}+\mathbf{s}_{11}-\mathbf{s}_{12}$	6
54	$\mathbf{s}_7+\mathbf{s}_8+\mathbf{s}_9+\mathbf{s}_{10}-2\mathbf{s}_{11}-2\mathbf{s}_{12}$	4
55	$3\mathbf{s}_6+3\mathbf{s}_7+3\mathbf{s}_8-4\mathbf{s}_{11}-8\mathbf{s}_{12}$	20
56	$4\mathbf{s}_6+4\mathbf{s}_7+4\mathbf{s}_8-3\mathbf{s}_{11}-9\mathbf{s}_{12}$	30
57	$\mathbf{s}_7+\mathbf{s}_8-\mathbf{s}_9-\mathbf{s}_{10}-\mathbf{s}_{11}-\mathbf{s}_{12}$	2
58	$\mathbf{s}_5+\mathbf{s}_6+\mathbf{s}_7+\mathbf{s}_8-\mathbf{s}_{11}-3\mathbf{s}_{12}$	2
59	$\mathbf{s}_8+\mathbf{s}_9-3\mathbf{s}_{10}-3\mathbf{s}_{11}+4\mathbf{s}_{12}$	12
60	$\mathbf{s}_7+\mathbf{s}_8-\mathbf{s}_{11}-\mathbf{s}_{12}$	4
61	$2\mathbf{s}_4+2\mathbf{s}_5+2\mathbf{s}_6-\mathbf{s}_{10}-\mathbf{s}_{11}-4\mathbf{s}_{12}$	6

Table 7: The basis junctions for $r=2$ (continued) and 1.

3.3.2 Case of non-Cartan type

In Table 2 there exists a class of $E(K)$ which are characterized by the intersection matrices of non-Cartan type (3.20). It is intriguing that we can indeed derive these intersection matrices from the junctions. Some examples are given as follows:

Example. (No.12)

We have the 7-branes $(\mathbf{A}^3)(\mathbf{A}^2)^2\mathbf{ABCBC}$. The junctions orthogonal to $T = A_2 \oplus A_1^{\oplus 2}$ are

$$\begin{aligned}
\mathbf{j}_1 &= \mathbf{s}_4 + \mathbf{s}_5 + 2\mathbf{s}_8 + \mathbf{s}_{10} - 2\mathbf{s}_{11} - 3\mathbf{s}_{12}, \\
\mathbf{j}_2 &= \mathbf{s}_6 + \mathbf{s}_7 - \mathbf{s}_{11} - \mathbf{s}_{12}, \\
\mathbf{j}_3 &= \mathbf{s}_{10} - \mathbf{s}_{12}, \\
\mathbf{j}_4 &= \mathbf{s}_4 + \mathbf{s}_5 - \mathbf{s}_{11} - \mathbf{s}_{12}.
\end{aligned} \tag{3.34}$$

These consist of the basis junctions of L. The intersection matrix turns out to be

$$-(\mathbf{j}_i, \mathbf{j}_j) = \begin{pmatrix} 4 & -1 & 0 & 1 \\ -1 & 2 & -1 & 0 \\ 0 & -1 & 2 & -1 \\ 1 & 0 & -1 & 2 \end{pmatrix}. \tag{3.35}$$

The inverse of this yields the matrix $\Lambda_{(12)}$ of (3.20).

Example. (No.17)

We have the 7-branes $(\mathbf{A}^5)(\mathbf{A}^2)\mathbf{ABCBC}$. The junctions orthogonal to $T = A_4 \oplus A_1$ are

$$\begin{aligned}
\mathbf{j}_1 &= 2\mathbf{s}_8 + \mathbf{s}_{10} - \mathbf{s}_{11} - 2\mathbf{s}_{12}, \\
\mathbf{j}_2 &= \mathbf{s}_6 + \mathbf{s}_7 - \mathbf{s}_{11} - \mathbf{s}_{12}, \\
\mathbf{j}_3 &= \mathbf{s}_{10} - \mathbf{s}_{12},
\end{aligned} \tag{3.36}$$

whose intersection matrix is

$$-(\mathbf{j}_i, \mathbf{j}_j) = \begin{pmatrix} 4 & -1 & 1 \\ -1 & 2 & -1 \\ 1 & -1 & 2 \end{pmatrix}. \tag{3.37}$$

The inverse of this yields the matrix $\Lambda_{(17)}$ of (3.20).

Example. (No.25)
We have the 7-branes $(\mathbf{A}^7)\mathbf{ABCBC}$. The junctions orthogonal to $T = A_6$ are

$$\begin{aligned} \mathbf{j}_1 &= 2\mathbf{s}_8 - \mathbf{s}_{11} - \mathbf{s}_{12}, \\ \mathbf{j}_2 &= \mathbf{s}_{10} - \mathbf{s}_{12}, \end{aligned} \tag{3.38}$$

whose intersection matrix reads

$$-(\mathbf{j}_i, \mathbf{j}_j) = \begin{pmatrix} 4 & -1 \\ -1 & 2 \end{pmatrix}. \tag{3.39}$$

The inverse of this yields the matrix $\Lambda_{(25)}$ of (3.20).

Further computations enable us to write down the basis junctions and their intersections for all the cases of non-Cartan type (3.20). The results are shown in Tables 4–7.

Finally, for the case of $\operatorname{rank} E(K) = 1$ (Nos. 43–61), the lattice L is one dimensional and we have determined its generator. The result is presented in Table 7. Thus, we have completed the construction of the lattice L listed in Table 2 in terms of string junctions, producing the classification Tables 3–7.

4 Weight lattice and torsions

4.1 Weak integrality of invariant charges

The Mordell-Weil group $E(K)$ consists of the free part $E(K)/E(K)_{\text{tor}}$ and the torsion part $E(K)_{\text{tor}}$. According to Theorem 9.2 in [11] the former should be isomorphic to the weight lattice L^* of $L = T^\perp$ in E_8.

We first would like to discuss the property of L^* in view of junctions. Naively, the weight junctions $\boldsymbol{\omega}_i$ can be obtained as the dual to the basis junctions $\mathbf{j}_i$, *i.e.* $\boldsymbol{\omega}_i = (C^{-1})_{ij}\mathbf{j}_j$, where C is the intersection matrix. Though the invariant charges Q_i of these dual basis junctions $\boldsymbol{\omega}_i$ are in general not integer, we can remedy this *partially* by adding null junctions.

Example. (No.25)
The basis junctions of L read

$$\mathbf{j}_1 = (0, 0, 0, 0, 0, 0, 0, -2, 0, 0, 1, 1),$$

$$\mathbf{j}_2 = (0,0,0,0,0,0,0,0,0,-1,0,1), \tag{4.1}$$

for which the dual basis junctions $\boldsymbol{\omega}_1, \boldsymbol{\omega}_2$ are obtained as

$$\begin{aligned}
\boldsymbol{\omega}_1 &= \frac{1}{7}\,(2\,\mathbf{j}_1 + \mathbf{j}_2 + 3\,\boldsymbol{\delta}_2) \\
&= (-\frac{3}{7},-\frac{3}{7},-\frac{3}{7},-\frac{3}{7},-\frac{3}{7},-\frac{3}{7},-\frac{3}{7},-1,3,2,-1,0), \\
\boldsymbol{\omega}_2 &= \frac{1}{7}\,(\mathbf{j}_1 + 4\,\mathbf{j}_2 + 5\,\boldsymbol{\delta}_2) \\
&= (-\frac{5}{7},-\frac{5}{7},-\frac{5}{7},-\frac{5}{7},-\frac{5}{7},-\frac{5}{7},-\frac{5}{7},-1,5,3,-2,0),
\end{aligned} \tag{4.2}$$

where $\boldsymbol{\delta}_2$ is given by (3.18).

Example. (No.7)

We have $L = D_4 \oplus A_1$. Since L is generated by (3.33), the basis of the weight lattice is found to be

$$\begin{aligned}
\boldsymbol{\omega}_1 &= (0,0,\frac{1}{2},\frac{1}{2},\frac{1}{2},\frac{1}{2},1,1,-3,-2,1,0), \\
\boldsymbol{\omega}_2 &= (0,0,1,1,1,1,1,1,-5,-3,2,0), \\
\boldsymbol{\omega}_3 &= (-\frac{1}{2},-\frac{1}{2},0,0,\frac{1}{2},\frac{1}{2},0,0,0,0,0,0), \\
\boldsymbol{\omega}_4 &= (-\frac{1}{2},-\frac{1}{2},\frac{1}{2},\frac{1}{2},0,0,0,0,0,0,0,0), \\
\boldsymbol{\omega}_5 &= (\frac{1}{2},\frac{1}{2},\frac{1}{2},\frac{1}{2},\frac{1}{2},\frac{1}{2},1,0,-3,-2,1,0).
\end{aligned} \tag{4.3}$$

These examples show that some of the charges Q_i still remain fractional. However, the fractionality is restricted by certain condition which we call *weak* integrality. In general, a junction orthogonal to the lattice T can be represented by using tadpole junctions ($\mathbf{J}_2$ in Figure 1) that go around the collapsed branes and do not touch them directly. Accordingly, for each of the collapsed branes, say $(\mathbf{X}_{[\mathbf{p_i},\mathbf{q_i}]} \cdots \mathbf{X}_{[\mathbf{p_j},\mathbf{q_j}]})$, we require the integrality not for *individual* charges Q_k $(i \le k \le j)$, but for their *total* (p,q) charges. Namely

$$(p,q) = Q_i(p_i,q_i) + \cdots + Q_j(p_j,q_j) \in \mathbf{Z}^2. \tag{4.4}$$

We call this condition *weak integrality*.

We now wish to point out that the junctions orthogonal to T subject to this weak integrality condition form the full Mordell-Weil lattice $E(K)$ rather than the lattice L

(called the narrow Mordell-Weil lattice in [11, 12]). To see this, we have first checked that the torsion free part of $E(K)$ is the dual lattice L^* of L by explicitly constructing the dual basis in terms of string junctions. The dual basis junctions have been worked out for all the cases Nos. 1–61. They indeed satisfy the weak integrality condition.

4.2 Torsions as fractional null junctions

Let us next consider the torsion part $E(K)_{\rm tor}$. By definition, a section $P \in E(K)$ is a torsion if and only if $mP = O$ for some $m \in \mathbf{Z}_{>0}$. Then its height pairing vanishes $(P, Q) = 0$ for any $Q \in E(K)$ since $m(P, Q) = (O, Q) = 0$. Hence P corresponds to a null junction. We know there are two independent null junctions $\boldsymbol{\delta}_1$, $\boldsymbol{\delta}_2$. By virtue of the Hanany-Witten effect, these null junctions can be transformed to the canonical form with integer charges Q_i, see (3.18) for instance. We call such null junctions strongly integral ones. As we remarked above, a fractional junction which is integral only in weak sense is also allowed for $E(K)$. It is then shown that the weakly integral null junctions, which we refer to as fractional loop junctions, are identified as the torsions (modulo strongly integral null junctions). Our idea is explained by presenting some examples explicitly.

Example. (No.73)

The brane configuration consists of two collapsed branes $(\mathbf{A}^4\mathbf{BC})(\mathbf{A}^4\mathbf{BC})$. Each of them supports one of the D_4 components in $T = D_4 \oplus D_4$. The junctions orthogonal to T become null junctions of the form

$$\begin{aligned} \mathbf{j} \;=\; & Q_1(\mathbf{s}_1 + \mathbf{s}_2 + \mathbf{s}_3 + \mathbf{s}_4) - (2Q_1 + Q_{12})\mathbf{s}_5 - Q_{12}\mathbf{s}_6 \\ & -Q_1(\mathbf{s}_7 + \mathbf{s}_8 + \mathbf{s}_9 + \mathbf{s}_{10}) + (2Q_1 + Q_{12})\mathbf{s}_{11} + Q_{12}\mathbf{s}_{12}. \end{aligned} \tag{4.5}$$

Thus the (p, q) charges exchanged between the two D_4 components are $p = 2(Q_1 - Q_{12})$ and $q = 2(Q_1 + Q_{12})$. The integrality condition on (p, q) requires $2Q_1 \equiv 2Q_{12} \equiv 0$. Hence we obtain the $(\mathbf{Z}/2\mathbf{Z})^2$ torsion. The generators of the torsion junctions are

$$\begin{aligned} \mathbf{j} &= (0,0,0,0,-\frac{1}{2},-\frac{1}{2},0,0,0,0,\frac{1}{2},\frac{1}{2}), \\ \mathbf{j}' &= (-\frac{1}{2},-\frac{1}{2},-\frac{1}{2},-\frac{1}{2},\frac{3}{2},\frac{1}{2},\frac{1}{2},\frac{1}{2},\frac{1}{2},\frac{1}{2},-\frac{3}{2},-\frac{1}{2}) \end{aligned} \tag{4.6}$$

which in fact obey $\mathbf{j}^2 = \mathbf{j}'^2 = 0$ and $2\,\mathbf{j} = \boldsymbol{\delta}_1$, $2\,\mathbf{j}' = \boldsymbol{\delta}_2$. They are represented as the

fractional loop junctions with the charges $(r,s)=(\frac{1}{2},0)$ for $\mathbf{j}$ and $(r,s)=(0,\frac{1}{2})$ for $\mathbf{j}'$.[‡]

Example. (No.66)

We have the 7-branes $(\mathbf{A}^6)(\mathbf{B}^3)(\mathbf{X}^2_{[\mathbf{1},-\mathbf{2}]})\mathbf{C}$ and the torsion group reads $\mathbf{Z}/6\mathbf{Z}$. This is generated by the torsion junction

$$\mathbf{j}=(-\frac{1}{6},-\frac{1}{6},-\frac{1}{6},-\frac{1}{6},-\frac{1}{6},-\frac{1}{6},\frac{2}{3},\frac{2}{3},\frac{2}{3},-\frac{1}{2},-\frac{1}{2},0) \tag{4.7}$$

which obeys $\mathbf{j}^2=0$ and $6\,\mathbf{j}=\boldsymbol{\delta}_1+\boldsymbol{\delta}_2$. As a fractional loop junction this carries the charges $(r,s)=(\frac{1}{6},\frac{1}{6})$.

Example. (No.74)

We have the 7-branes $(\mathbf{A}^4)(\mathbf{B}^4)(\mathbf{X}^2_{[\mathbf{0},\mathbf{1}]})(\mathbf{X}^2_{[\mathbf{2},\mathbf{1}]})$ and the torsion group reads $\mathbf{Z}/4\mathbf{Z}\oplus\mathbf{Z}/2\mathbf{Z}$. This is generated by the torsion junctions

$$\begin{aligned}\mathbf{j}&=(-\frac{1}{4},-\frac{1}{4},-\frac{1}{4},-\frac{1}{4},\frac{3}{4},\frac{3}{4},\frac{3}{4},\frac{3}{4},2,2,-\frac{1}{2},-\frac{1}{2}),\\ \mathbf{j}'&=(0,0,0,0,-\frac{1}{2},-\frac{1}{2},-\frac{1}{2},-\frac{1}{2},-\frac{3}{2},-\frac{3}{2},\frac{1}{2},\frac{1}{2})\end{aligned} \tag{4.8}$$

which obey $\mathbf{j}^2=\mathbf{j}'^2=0$ and $4\,\mathbf{j}=\boldsymbol{\delta}_2$, $2\,\mathbf{j}'=\boldsymbol{\delta}_1$. As fractional loop junctions they carry the charges $(r,s)=(0,\frac{1}{4})$ for $\mathbf{j}$ and $(r,s)=(\frac{1}{2},0)$ for $\mathbf{j}'$.

Following this procedure we can express the generators of all the torsion groups in Table 2 as the fractional loop junctions with the (r,s) charges. Our result is

$\mathbf{Z}/2\mathbf{Z}:\ (r,s)=(\frac{1}{2},\frac{1}{2})$ Nos. 13, 21, 28, 34, 35, 38, 44, 48, 53, 54, 59, 64, 65.

$\mathbf{Z}/2\mathbf{Z}:\ (r,s)=(0,\frac{1}{2})$ No. 24.

$\mathbf{Z}/2\mathbf{Z}:\ (r,s)=(\frac{1}{2},0)$ Nos. 41, 52.

$\mathbf{Z}/3\mathbf{Z}:\ (r,s)=(\frac{1}{3},\frac{1}{3})$ Nos. 39, 51, 61, 63.

$\mathbf{Z}/3\mathbf{Z}:\ (r,s)=(0,\frac{1}{3})$ No. 69.

$\mathbf{Z}/4\mathbf{Z}:\ (r,s)=(\frac{1}{4},\frac{1}{4})$ Nos. 58, 70.

$\mathbf{Z}/4\mathbf{Z}:\ (r,s)=(\frac{1}{4},\frac{1}{2})$ No. 72.

$\mathbf{Z}/5\mathbf{Z}:\ (r,s)=(\frac{1}{5},\frac{1}{5})$ No. 67.

$\mathbf{Z}/6\mathbf{Z}:\ (r,s)=(\frac{1}{6},\frac{1}{6})$ No. 66.

$(\mathbf{Z}/2\mathbf{Z})^2:\ (r,s)=(\frac{1}{2},0),(0,\frac{1}{2})$ Nos. 42, 57, 60, 71, 73.

$(\mathbf{Z}/3\mathbf{Z})^2:\ (r,s)=(\frac{1}{3},0),(0,\frac{1}{3})$ No. 68.

[‡]We note again that the charges Q_i for $\boldsymbol{\delta}_1,\boldsymbol{\delta}_2$ depend on the brane configurations.

$\mathbf{Z}/4\mathbf{Z} \oplus \mathbf{Z}/2\mathbf{Z}$: $(r,s) = (0,\frac{1}{4}), (\frac{1}{2},0)$ No. 74.

The result for the torsion group we have obtained from the junction consideration is in agreement with that in [12].

5 Discussion

In this paper, we have systematically studied the structure of singularities, Mordell-Weil lattices and torsions of a rational elliptic surface by making use of the 7-brane-junction technology. Our results are in nice agreement with Oguiso-Shioda's Main Theorem in [12]. Consequently we found explicit correspondence between sections and junctions, which is summarized in Table 8.

Though we have restricted ourselves to the case of rational elliptic surfaces, generalization to other elliptic surfaces is clear and stated as follows:[§] For a general elliptic surface $p : S \to C$ over a curve C, the lattice of strongly integral tadpole junctions can be identified with the cohomology group $H^1(C, R^1p_*\mathbf{Z})$ whose $H^{1,1}$ part is isomorphic to the narrow Mordell-Weil group of S. (For a rational elliptic surface, all the elements in $H^1(C, R^1p_*\mathbf{Z})$ belong to its $H^{1,1}$ part, however, it is not so in general.) Since the sheaf $R^1p_*\mathbf{Z}$ is a local system whose fiber at $x \in C$ is $H^1(p^{-1}(x), \mathbf{Z}) = \mathbf{Z}\alpha \oplus \mathbf{Z}\beta$, the cohomology $H^1(C, R^1p_*\mathbf{Z})$ can be evaluated by using group cohomology associated with the monodromy representation $\rho : \pi_1(C - \{\text{singularity}\}) \to SL(2,\mathbf{Z})$. The 7-brane-junction technology may offer an efficient way to calculate this cohomology $H^1(C, R^1p_*\mathbf{Z})$ and intersections on it.

One may apply our results to gain a physical understanding of torsion groups which play an important role to determine the gauge *group* rather than the gauge *algebra* [10]. Since the structure of Mordell-Weil lattices is related to the Wilson lines on the heterotic side under F-theory/heterotic duality, it will be interesting to think of the issue from the heterotic string point of view.

Another application is found when we consider stable non-BPS states in F-theory. It has recently been recognized that, in string theory, there exist solitonic states which are stable but not BPS [24]. These states are the lightest ones which carry certain conserved

[§]We thank M. Saito for pointing out this interpretation. See [23].

	section	junction
O	zero section	strongly integral null junctions
$E(K)_{\rm tor}$	torsions	weakly integral null junctions
L	narrow Mordell-Weil lattice	strongly integral tadpole junctions
$E(K)$	Mordell-Weil lattice	weakly integral tadpole junctions

Table 8: Sections and junctions

charges, *i.e.* there exist no other BPS or non-BPS states of lower mass having the same charges. Thus their stability is ensured by charge conservation. In [2] the analysis of stable non-BPS states in F-theory on $K3$ was initiated. As we will see now, the structure of the Mordell-Weil lattice determines the 7-brane configurations supporting non-BPS junctions which could be candidates for stable non-BPS states in a region of the moduli space of F-theory on $K3$.

Let us consider the region of the moduli space where 24 7-branes for an elliptic $K3$ are split into two $\widehat{\mathbf{E}}_9$ [6]. This corresponds to the so-called stable degeneration of $K3$ [7, 8]. Two $\widehat{\mathbf{E}}_9$ brane configurations are properly isolated from each other in the sense of [2]. Thus we may focus on string junctions stretched on a single $\widehat{\mathbf{E}}_9$ to analyze non-BPS states. The BPS junctions $\mathbf{J}_{BPS}$ have to obey the holomorphy condition which is stated as $\mathbf{J}_{BPS}^2 \geq -2$ [25, 26]. Thus junctions $\mathbf{J}$ with $\mathbf{J}^2 < -2$ are non-BPS. Inspecting Table 7 we first observe that the basis junctions of one-dimensional L, except for the case $L = A_1$, are all non-BPS. As for the higher rank $E(K)$, we also have non-BPS basis junctions in Nos. 12, 17, 19, 20, 22, 23, 25, 29–33, 36–38, 40 and 41. We note that the cases No.45 ($\widehat{\widehat{\mathbf{E}}}_1$), No.46 ($\mathbf{D}_1$) and No.25 ($\widetilde{\mathbf{E}}_2$) have already appeared in [2]. Each non-BPS basis junction, which we denote as $\mathbf{j}_{u(1)}$, generates the $U(1)$ symmetry associated to the one-dimensional lattice. It is clear that any junction can be written as

$$\mathbf{J} = \mathbf{j}^{\perp} + n\,\mathbf{j}_{u(1)}, \tag{5.1}$$

where $n \in \mathbf{Z}$ and $\mathbf{j}^{\perp}$ stands for the orthogonal components of $\mathbf{J}$ with respect to the $U(1)$ direction. Then the self-intersection is obtained as $\mathbf{J}^2 = \mathbf{j}^{\perp\,2} + n^2\,\mathbf{j}_{u(1)}^2$. Since $\mathbf{j}^{\perp\,2} \leq 0$ and

$\mathbf{j}_{u(1)}^2 < -2$ we have $\mathbf{J}^2 < -2$ for any $n \neq 0$. Therefore the junctions with non-vanishing component along $\mathbf{j}_{u(1)}$ represent non-BPS states. Among these non-BPS states there could be stable states against decay. Identifying such stable states requires the detailed dynamical analysis which is beyond the scope of this paper.

Acknowledgements

We would like to thank M. Noumi and M. Saito for valuable discussions. We also wish to thank K. Oguiso for ascertaining some corrections in the Table in [12] and Y. Ohtake for preparing figures in this paper. The work of SKY was supported in part by Grant-in-Aid for Scientific Research on Priority Area 707 "Supersymmetry and Unified Theory of Elementary Particles", Japan Ministry of Education, Science and Culture.

References

[1] Y. Yamada and S.-K. Yang, *Affine 7-brane Backgrounds and Five-Dimensional E_N Theories on S^1*, hep-th/9907134.

[2] A. Sen and B. Zwiebach, *Stable Non-BPS States in F-theory*, hep-th/9907164.

[3] C. Vafa, *Evidence for F-Theory*, Nucl. Phys. **B469** (1996) 403, hep-th/9602022.

[4] A. Sen, *F-theory and Orientifolds*, Nucl. Phys. **B475** (1996) 562, hep-th/9605150.

[5] D.R. Morrison and C. Vafa, *Compactifications of F-Theory on Calabi–Yau Threefolds – I*, Nucl. Phys. **B473** (1996) 74-92, hep-th/9602114;
Compactifications of F-Theory on Calabi–Yau Threefolds – II, Nucl. Phys. **B476** (1996) 437, hep-th/9603161.

[6] O. DeWolfe, T. Hauer, A. Iqbal and B. Zwiebach, *Uncovering Infinite Symmetries on $[p, q]$ 7-branes: Kac-Moody Algebras and Beyond*, hep-th/9812209.

[7] R. Friedman, J. Morgan and E. Witten, *Vector Bundles and F Theory*, Commun. Math. Phys. **187** (1997) 679, hep-th/9701162.

[8] P.S. Aspinwall and D.R. Morrison, *Point-like Instantons on K3 Orbifolds*, Nucl. Phys. **B503** (1997) 533, hep-th/9705104.

[9] P.S. Aspinwall, *Aspects of the Hypermultiplet Moduli Space in String Duality*, JHEP **9804** (1998) 019, hep-th/9802194.

[10] P.S. Aspinwall and D.R. Morrison, *Non-Simply-Connected Gauge Groups and Rational Points on Elliptic Curves*, JHEP **9807** (1998) 012, hep-th/9805206.

[11] T. Shioda, *On the Mordell-Weil Lattices*, Comment. Math. Univ. St. Pauli. **39** (1990) 211.

[12] K. Oguiso and T. Shioda, *The Mordell-Weil Lattice of a Rational Elliptic Surface*, Comment. Math. Univ. St. Pauli. **40** (1991) 83.

[13] J.H. Silverman and J. Tate, *Rational Points on Elliptic Curves*, Undergraduate Texts in Mathematics, Springer-Verlag, 1992.

[14] K. Kodaira, *On Compact Analytic Surfaces II*, Ann. Math. **77** (1963) 563;
On Compact Analytic Surfaces III, Ann. Math. **78** (1963) 1.

[15] N. Seiberg and E. Witten, *Monopoles, Duality and Chiral Symmetry Breaking in N=2 Supersymmetric QCD*, Nucl. Phys. **B431** (1994) 484, hep-th/9408099.

[16] J.A. Minahan and D. Nemeschansky, *An N=2 Superconformal Fixed Point with E_6 Global Symmetry*, Nucl. Phys. **B482** (1996) 142, hep-th/9608047;
Superconformal Fixed Points with E_n Global Symmetry, Nucl. Phys. **B489** (1997) 24, hep-th/9610076.

[17] M. Noguchi, S. Terashima and S.-K. Yang, *N=2 Superconformal Field Theory with ADE Global Symmetry on a D3-brane Probe*, hep-th/9903215, to appear in Nucl. Phys. **B**.

[18] J.A. Minahan, D. Nemeschansky and N.P. Warner, *Investigating the BPS Spectrum of Non-Critical E_n Strings*, Nucl. Phys. **B508** (1997) 64, hep-th/9705237.

[19] O. DeWolfe and B. Zwiebach, *String Junctions for Arbitrary Lie Algebra Representations*, Nucl. Phys. **B541** (1999) 509, hep-th/9804210.

[20] O. DeWolfe, T. Hauer, A. Iqbal and B. Zwiebach, *Uncovering the Symmetries on $[p,q]$ 7-branes: Beyond the Kodaira Classification*, hep-th/9812028.

[21] M.R. Gaberdiel, T. Hauer and B. Zwiebach, *Open string - string junction transitions*, Nucl. Phys. **B525** (1998) 117, hep-th/9801205.

[22] R. Miranda, *The Moduli of Weierstrass fibrations over $\mathbf{P}^1$*, Math. Ann. **255** (1981) 379.

[23] D. Cox and S. Zucker, *Intersection numbers of sections of elliptic surfaces*, Invent. Math. **53** (1979) 1.

[24] A. Sen, *Stable Non-BPS States in String Theory*, JHEP **9806** (1998) 007, hep-th/9803194;
Stable Non-BPS Bound States of BPS D-branes, JHEP **9808** (1998) 010, hep-th/9805019.

[25] A. Mikhailov, N. Nekrasov and S. Sethi, *Geometric Realizations of BPS States in N=2 Theories*, Nucl. Phys. **B531** (1998) 345, hep-th/9803142.

[26] O. DeWolfe, T. Hauer, A. Iqbal and B. Zwiebach, *Constraints on the BPS Spectrum of N = 2, D = 4 Theories with A-D-E Flavor Symmetry*, Nucl. Phys. **B534** (1998) 261, hep-th/9805220.